

SANDIA REPORT

SAND2003-2917

Unlimited Release

Printed September 2003

Diagnostics Development Plan for ZR

David L. Hanson

Prepared by
Sandia National Laboratories
Albuquerque, New Mexico 87185 and Livermore, California 94550

Sandia is a multiprogram laboratory operated by Sandia Corporation,
a Lockheed Martin Company, for the United States Department of Energy's
National Nuclear Security Administration under Contract DE-AC04-94AL85000.

Approved for public release; further dissemination unlimited.



Issued by Sandia National Laboratories, operated for the United States Department of Energy by Sandia Corporation.

NOTICE: This report was prepared as an account of work sponsored by an agency of the United States Government. Neither the United States Government, nor any agency thereof, nor any of their employees, nor any of their contractors, subcontractors, or their employees, make any warranty, express or implied, or assume any legal liability or responsibility for the accuracy, completeness, or usefulness of any information, apparatus, product, or process disclosed, or represent that its use would not infringe privately owned rights. Reference herein to any specific commercial product, process, or service by trade name, trademark, manufacturer, or otherwise, does not necessarily constitute or imply its endorsement, recommendation, or favoring by the United States Government, any agency thereof, or any of their contractors or subcontractors. The views and opinions expressed herein do not necessarily state or reflect those of the United States Government, any agency thereof, or any of their contractors.

Printed in the United States of America. This report has been reproduced directly from the best available copy.

Available to DOE and DOE contractors from

U.S. Department of Energy
Office of Scientific and Technical Information
P.O. Box 62
Oak Ridge, TN 37831

Telephone: (865)576-8401
Facsimile: (865)576-5728
E-Mail: reports@adonis.osti.gov
Online ordering: <http://www.doe.gov/bridge>

Available to the public from

U.S. Department of Commerce
National Technical Information Service
5285 Port Royal Rd
Springfield, VA 22161

Telephone: (800)553-6847
Facsimile: (703)605-6900
E-Mail: orders@ntis.fedworld.gov
Online order: <http://www.ntis.gov/help/ordermethods.asp?loc=7-4-0#online>



SAND2003-2917
Unlimited Release
Printed September 2003

Diagnostics Development Plan for ZR

David L. Hanson
Z-Pinch Experiments and Advanced Diagnostics
Sandia National Laboratories
P. O. Box 5800
Albuquerque, NM 87185-1193

Revised April 2003

Abstract

The Z Refurbishment (ZR) Project is a program to upgrade the Z machine at SNL with modern durable pulsed power technology, providing additional shot capacity and improved reliability as well as advanced capabilities for both pulsed x-ray production and high pressure generation. The development of enhanced diagnostic capabilities is an essential requirement for ZR to meet critical mission needs. This report presents a comprehensive plan for diagnostic instrument and infrastructure development for the first few years of ZR operation. The focus of the plan is on: (1) developing diagnostic instruments with high spatial and temporal resolution, capable of low noise operation and survival in the severe EMP, bremsstrahlung, and blast environments of ZR; and (2) providing diagnostic infrastructure improvements, including reduced diagnostic trigger signal jitter, more and flexible diagnostic line-of-sight access, and the capability for efficient exchange of diagnostics with other laboratories. This diagnostic plan is the first step in an extended process to provide enhanced diagnostic capabilities for ZR to meet the diverse programmatic needs of a broad range of defense, energy, and general science programs of an international user community into the next decade.

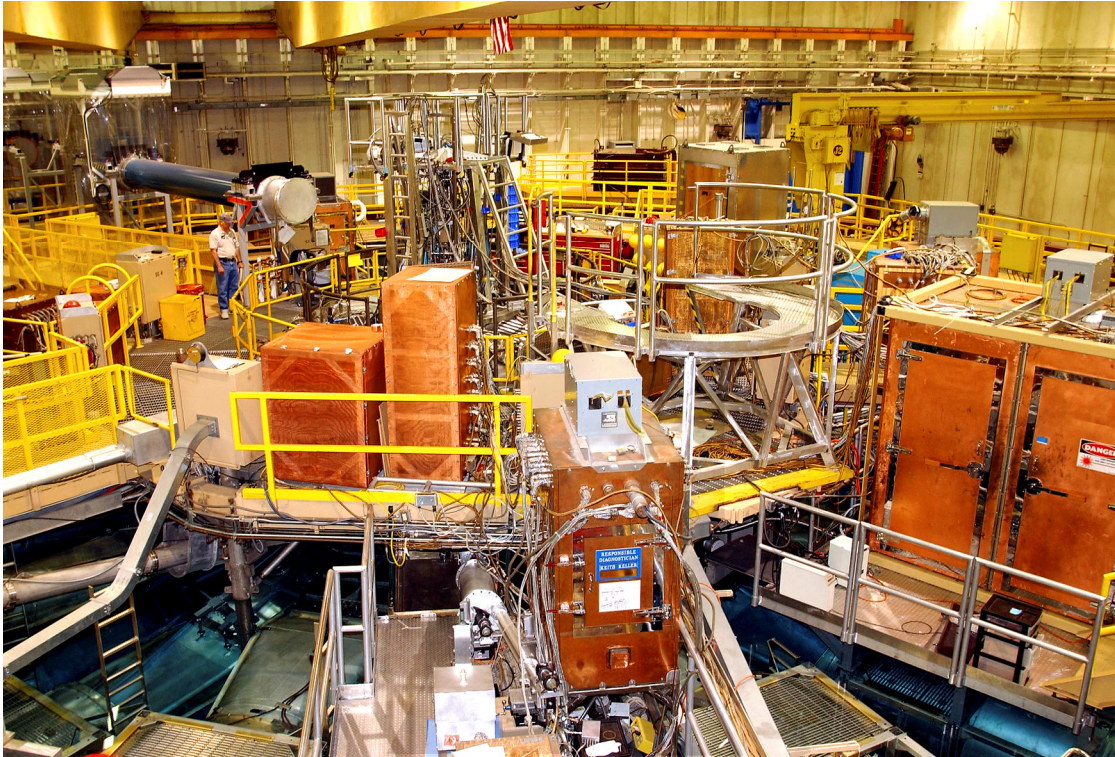
Acknowledgements

The author would like to thank James R. Asay, James E. Bailey, Guy R. Bennett, David E. Bliss, Gordon A. Chandler, Robert E. Chrien (LANL), Michael E. Cuneo, Jean-Paul Davis, Christopher Deeney, Michael D. Furnish, Clint A. Hall, Robert F. Heeter (LLNL), Randy J. Hickman, Daniel O. Jobe, Robert R. Johnston, Marcus D. Knudson, Ramon J. Leeper, Barbara A. Lewis, Michael G. Mazarakis, M. Keith Matzen, Dillon H. McDaniel, Thomas A. Mehlhorn, Jerry A. Mills, Thomas J. Nash, Dan S. Nielsen, Donald W. Petmecky, John L. Porter, Jr., David B. Reisman (LLNL), Gregory A. Rochau, Stephen D. Rothman (AWE), Laurence E. Ruggles, Carlos L. Ruiz, Johann F. Seamen, Thomas W. L. Sanford, Walter W. Simpson, Daniel B. Sinars, C. Shane Speas, William A. Stygar, Mary Ann Sweeney, Jose A. Torres, Robert G. Watt (LANL), Edward A. Weinbrecht, and David F. Wenger for many valuable suggestions and insights on the requirements for ZR diagnostic and infrastructure development.

Contents

Executive Summary	9
I. Introduction	11
II. New Diagnostics for ZR	13
II.1. Introduction	13
II.2. Z-Beamlet Backlighter Diagnostic System	13
II.3. Monochromatic Imaging of Z Pinches	18
II.4. High Spatial Resolution X-ray Pinhole Cameras	19
II.5. Spectroscopy Diagnostics	19
II.6. Thomson Scattering Diagnostic	21
II.7. Extended Range Soft X-ray Spectrometer	21
II.8. Hard X-ray Spectrometer	21
II.9. Neutron Diagnostics	22
II.10. VISAR System Development	26
II.11. Imaging Shock Breakout Diagnostic	26
II.12. Laser Plasma Probes	26
II.13. Pulsed Power Flash Radiography System	27
II.14. Visible Imaging Hydrotest Capability	27
III. Improvements to Existing Diagnostics for ZR	28
III.1. Introduction	28
III.2. Upgrade of the LOS 5/6 Diagnostics Package	28
III.3. Improved Load Current Monitors	30
III.4. Large Format Framing Camera	31
III.5. Active Shock Breakout (ASBO) Diagnostic	31
III.6. Time-resolved X-ray Crystal Spectrometer	31
III.7. Replacement of Standard Convex Crystal Spectrometers with Elliptical Analyzers	32
III.8. Additional TREX Instruments	32
III.9. Calibrated Streak Camera Systems	32
III.10. Improved Diagnostic Request Form	33
IV. Diagnostic Infrastructure and Operational Issues for ZR	34
IV.1. Introduction	34
IV.2. Redesign of Diagnostic Platform and Boat Structures	34
IV.3. Centralized Screen Boxes	34
IV.4. Radial LOS Access	37
IV.5. Digital Insertion Manipulators (DIMs)	39
IV.6. Extension of Radial LOS Pipe Lengths	40
IV.7. Axial LOS Access Issues	41

IV.8. On-Axis Debris Mitigation	44
IV.9. Target Chamber Vacuum Feedthrough Ports	44
IV.10. Diagnostic Timing	45
IV.11. Vacuum System Issues	46
IV.12. Diagnostic Operational Issues	47
IV.13. Remote Control of Diagnostics	47
IV.14. Fiber-coupled Vacuum Illumination Systems	47
IV.15. Improved Diagnostic Turn-around Time	48
IV.16. Center Section Mock-up	48
IV.17. Tritium Use on ZR	48
IV.18. DAS Screenroom Space Utilization	48
IV.19. Conceptual Design Study for ZR Double-Sided-Drive Configuration	49
IV.20. Conceptual Design Study for Petawatt Laser Compatibility ...	50
V. Diagnostics Calibration and Data Analysis Issues for ZR	51
V.1. Introduction	51
V.2. Calibration of Z-pinch X-ray Energy and Power Diagnostics	51
V.3. X-ray Crystal Calibration and Characterization	52
V.4. Pulsed Laser X-ray Calibration Source	53
V.5. MCP Characterization	53
V.6. X-ray Film Calibration	53
V.7. Searchable Data Base for ZR Shots	53
V.8. Data Analysis Procedures	54
VI. Priorities and Budget	55
VI.1. Prioritized List of Recommendations	55
VI.2. Budget for New Diagnostic Development	58
VII. Summary and Conclusions	59
Acknowledgements	59
References	60
Appendix A. Summary of Z Core Diagnostics	66
A1. List of Radial (12°) Diagnostics	66
A2. List of Axial Diagnostics	66
A3. List of Target Chamber (Close-in) Diagnostics	67
A4. List of Electrical Power Flow Diagnostics	67
A5. Brief Description of Diagnostics	68



List of Figures

Fig. 1. Scope of ZR Project pulsed power development	12
Fig. 2. ZBL layout	14
Fig. 3. ZBL Facility	14
Fig. 4. ZBL beam transport to Z	15
Fig. 5. ZBL beam transport and off-axis FOA for PPI	16
Fig. 6. ZBL point-projection backlighting of capsule.....	17
Fig. 7. Low-threshold neutron yield detector	22
Fig. 8. Neutron TOF diagnostic on LOS 25/26	24
Fig. 9. LOS 5/6 pipe and vacuum system.....	29
Fig. 10. TGS on LOS 5/6	30
Fig. 11. LOS 17/18 and LOS 21/22 screen boxes.....	33
Fig. 12. Medium-sized walk-in screen room	36
Fig. 13. LOS 1/2 radial LOS pipes	37
Fig. 14. LOS 29/30 diagnostics	38
Fig. 15. NIF DIM	39
Fig. 16. Axial diagnostics package.....	41
Fig. 17. Axial diagnostics	42
Fig. 18. Bottom axial diagnostics package.....	43
Fig. 19. Bottom axial x-ray PHC	43

Executive Summary

The Z Refurbishment (ZR) Project is a program to upgrade the Z machine at SNL with modern, durable pulsed power technology. This will provide additional shot capacity and reliability, as well as significantly increased capability, enhanced precision and pulse shaping variability, and the flexibility to adapt to the changing requirements of future experimental needs. This major upgrade will allow ZR to provide critical capabilities and unique data to support stockpile stewardship, high energy density physics, inertial confinement fusion (ICF), dynamic materials properties, and basic science research into the next decade.

An essential element of the ZR Project and associated activities will be the development of enhanced diagnostics that can fully utilize the x-ray and high pressure generation capabilities of ZR at an increased shot rate. The purpose of this study is to identify and prioritize the new and improved diagnostic capabilities and to present the results in the form of an initial development plan focusing on diagnostic needs for the first few years of ZR operation.

A primary goal of the ZR Project is to develop standardized access and supporting infrastructure for efficient, reliable operation of an enhanced group of core plasma, neutron, and shock physics diagnostics. Proposed developments include a redesign of the diagnostic platform structure, use of large centralized screen boxes with standardized utilities, and an increase in radial line-of-sight access to permit flexibility in the location and number of diagnostic instruments fielded. Two DIM (Diagnostic Insertion Manipulator) modules should be developed with compatible radial diagnostic ports to encourage active collaboration with other laboratories through the efficient exchange of diagnostics. Machine command timing jitter must be reduced to ± 1 ns with respect to peak radiation power to synchronize early laser and diagnostic trigger signals with transient events, such as fast ignitor fuel assembly and x-ray photoionization, occurring in a narrow time window. The capability should be developed to maintain diagnostic cross-timing accuracies within ± 50 ps on these experiments. Conceptual design studies should evaluate the possible future adaptation of ZR and associated diagnostic access for double-sided power feed high yield and fast ignitor assessments.

Diagnostic infrastructure improvements and enhanced operational precision will provide support for increasingly sophisticated diagnostics with the improved time and spatial resolution required for a wide range of complex physics experiments. The focus must be on developing survivable instruments capable of operating at low noise levels in the severe electro-magnetic pulse (EMP) and bremsstrahlung radiation environment of ZR. High spatial and temporal resolution x-ray framing pinhole cameras and spectroscopy instruments will be required, and spectral coverage should be extended. New diagnostics are proposed to utilize the full capabilities of the Z Beamlet Laser (ZBL) backlighter system for point-projection x-ray backlighting, monochromatic x-ray imaging, and x-ray spectroscopy. Characterization of thermonuclear neutron yields from ICF capsule implosion experiments will require the progressive development of survivable, low threshold instruments for total neutron yield, neutron time-of-flight, target thermonuclear emission history and bang time, fuel areal density $\langle \rho r \rangle$, and neutron core image measurements. The development of single-point, line, and full-field VISAR interferometry systems with improved time resolution for dynamic materials properties

studies is already in progress. In addition to the development of new ZR diagnostics, a program is underway to improve the range, operation, reliability, calibration, alignment, data quality, and other essential features of diagnostics already in use on Z that will form the core diagnostic packages on ZR.

The ZR Diagnostics Development Plan in this report is based on ideas gathered from a large group of Z experimenters from SNL, LANL, LLNL, and AWE, with the intent of making ZR a national user facility that meets the programmatic needs of a broad range of outside users. This effort to formulate a diagnostic plan is the first step in an extended process that should result, on a 4-6 year timescale, in an enhanced set of diagnostic capabilities for ZR.



I. Introduction

The Z accelerator [1] is a pulsed-power-based current driver (20 MA) producing energetic (1.6 MJ), intense (>200 TW) pulsed x-ray sources and magnetically-generated high pressure pulses. Z provides critical capabilities and unique data to meet the requirements of the Stockpile Stewardship Program, and the High Energy Density Physics (HEDP), Secondary Certification, Nuclear Survivability, and Dynamic Materials Properties campaigns [2]. Current-driven wire array z-pinch implosions on Z generate intense x-ray pulses for radiation effects testing, radiation transport and hydrodynamics experiments, and indirect-drive ICF experiments. High-current-density short circuit geometries have been developed to provide magnetically-driven high pressure capabilities for Isentropic Compression Experiments (ICE) and the launching of hypervelocity flyer plates in support of dynamic material properties and equation-of-state (EOS) experiments. Z has become a fully utilized primary facility of the HEDP community, but reliability and operational issues resulting from the age of the machine make a significant upgrade to Z necessary if it is to continue to provide vital data for another decade [3]. This situation was recognized in the recent Mission Need Approval for the ZR Project by NNSA following a CD-0 review.

The goal of the Z Refurbishment (ZR) Project is to upgrade the Z machine with modern, durable technology (Fig. 1) to provide additional shot capacity and reliability as well as significantly increased capability, enhanced precision and pulse shaping variability, and the flexibility to adapt to the requirements of future experimental programs [4]. A primary objective of the ZR Project is to provide additional shot capacity, with component reliability and infrastructure to enable 400 shot opportunities per year if full double-shift operation is funded. A significant improvement in machine capabilities is also a primary criteria. Enhanced drive parameters include an increase in current to 26 MA into a standard z-pinch load for higher hohlraum temperatures and to 28-30 MA into a short circuit load configuration for higher magnetically-generated pressures. Enhanced precision and reproducibility of current pulses, improved timing jitter, and advanced pulse-shaping capabilities are also primary criteria for ZR [3]. Conceptual design and engineering support should also be provided to evaluate the feasibility of efficient and cost effective future adaptation of ZR to assess the double-sided power feed for high yield and to assess the fast ignition concept for ICF.

The development of enhanced diagnostic capabilities is also an essential requirement for ZR to meet critical mission needs. Among the primary criteria to be realized as part of the ZR Project will be the development of standardized access and supporting infrastructure for efficient and reliable operation of an enhanced group of core plasma, neutron, and shock physics diagnostics, enabling full utilization of the advanced source capabilities of ZR at an increased shot rate [3]. Diagnostic infrastructure improvements and enhanced operational precision will provide support for increasingly sophisticated diagnostics with improved time and spatial resolution required to do breakthrough physics experiments on ZR. The recently completed ZBL diagnostic system [5] represents a unique capability that will be fully utilized on ZR only through the development of appropriate new diagnostics and infrastructure. In developing new diagnostic capabilities for ZR, the experimental and programmatic requirements of other user organizations, such as LANL, LLNL, DTRA, and AWE, must be considered so that

ZR can be operated as an international user facility, serving the diverse needs of a broad range of defense, energy, and basic science programs. While the development of much of the ZR diagnostic infrastructure will be supported within the ZR Project itself, the development of new diagnostics will be carried out independently of the ZR Project, but with a strong focus on integrating ZR diagnostic development and diagnostic interface requirements and on defining ZR diagnostic interface needs with a long-term perspective.

The goal of the present study is to identify and prioritize new and improved diagnostic capabilities required for the technical excellence of experiments utilizing the enhanced pulsed power technology on ZR. Diagnostic instruments, infrastructure, and operations requirements are considered in subsequent sections of this report, with emphasis on the requirements, cost, and development time to field an enhanced set of diagnostics to meet critical mission needs for the first few years of ZR operation. This plan was assembled from information, ideas, and opinions collected from a large number of SNL experimenters and diagnostic technologists, and from the principal LANL, LLNL, and AWE users of Z. This ZR Diagnostic Development Plan should be considered a first step in an extended process of detailed design definition leading, on a 4-6 year time scale, to enhanced diagnostic capabilities to meet the exciting new experimental challenges on ZR.

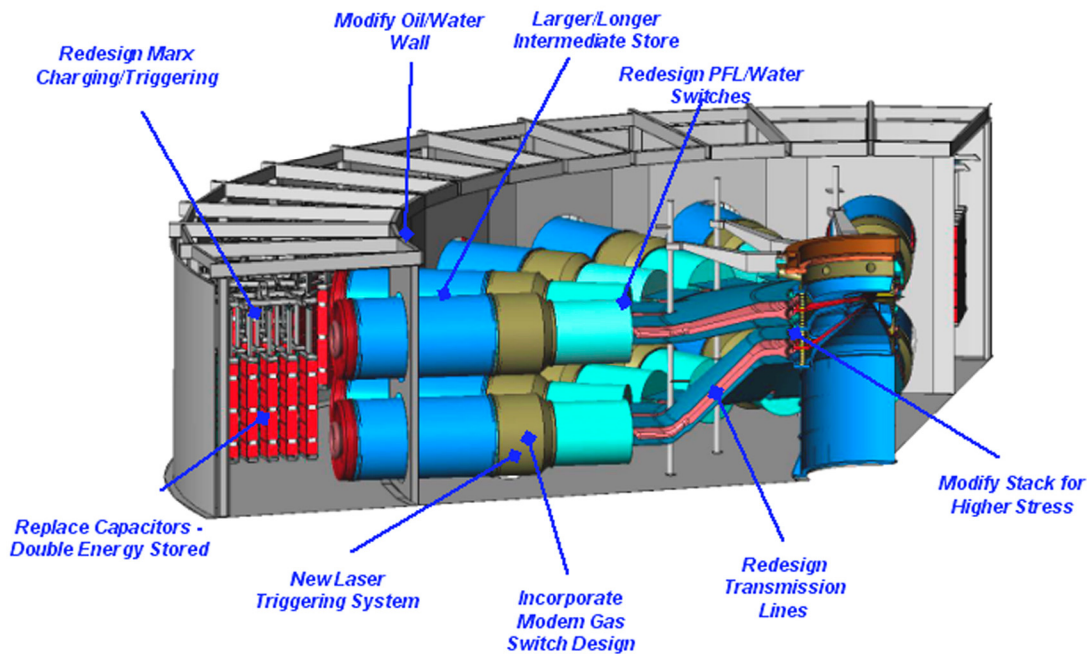


Fig. 1. Scope of the ZR Project pulsed power development.

II. New Diagnostics for ZR

II.1. Introduction

The enhanced capabilities of ZR for x-ray production and magnetic pressure generation will open new possibilities for weapons physics, high energy density physics, and dynamic materials properties research, requiring new and improved diagnostics. The main emphasis in a ZR diagnostics development program should be on providing survivable instruments capable of operating at low noise levels in the ZR bremsstrahlung and EMP environment with much improved spatial and time resolution, higher sensitivity, and improved dynamic range compared to the present diagnostics on Z. New diagnostics will be required to utilize the full capabilities of the Z-Beamlet backlighter as an intense point projection radiography source for ICF capsule implosion imaging, as an x-ray source for spectroscopy, and for other applications that will make it a primary diagnostic on ZR experiments. Higher drive temperatures and significant fusion neutron yields anticipated on ZR will result in increasing emphasis on neutron measurements to diagnose ICF fuel capsule implosion behavior.

Infrastructure developments will play an important role in exploiting new diagnostic capabilities. There is a critical need for increased flexibility in diagnostic line-of-sight (LOS) access to permit the fielding of both new and existing diagnostics at multiple locations and to provide adequate neutron diagnostic access. The increased focus on recording transient events in a narrow time window with much improved time resolution will require significant improvements in diagnostic timing jitter and the development of multiframe imaging capability in new instruments.

Specific recommendations for development of new diagnostic instruments for ZR are presented in this section. Diagnostic interface issues and infrastructure developments are discussed in more detail in Sec. IV.

II.2. Z-Beamlet Backlighter Diagnostic System

The Z-Beamlet laser backlighter system (Figs. 2-4) is a new diagnostic tool with wide application to experiments on ZR [5]. ZBL has recently become operational and is being used to produce 500 J of 2ω ($\lambda = 527$ nm) laser energy in a single pulse focused to a 50-100 μm diameter spot to generate 6.7-keV x rays for point projection imaging of ICF capsule implosions over a 4-mm-diameter field of view [6,7]. A heavily-shielded, low-noise, film-based x-ray detector has been developed to record radiographs of implosion capsules. An electromagnetically-driven shutter protects the film from debris [8].

ZBL diagnostic development activities over the next 4 years (FY03-06) will include expanding the Beamlet laser operating parameters to meet full design specifications and developing detector systems and infrastructure for a wide variety of additional applications. Example applications include x-ray imaging and microscopy of ICF targets in z-pinch-driven hohlraums (ZPDH) [9-11] and dynamic hohlraums (DH) [12,13], backlighting of radiation-driven and magnetically-driven experiments, and spectroscopy.

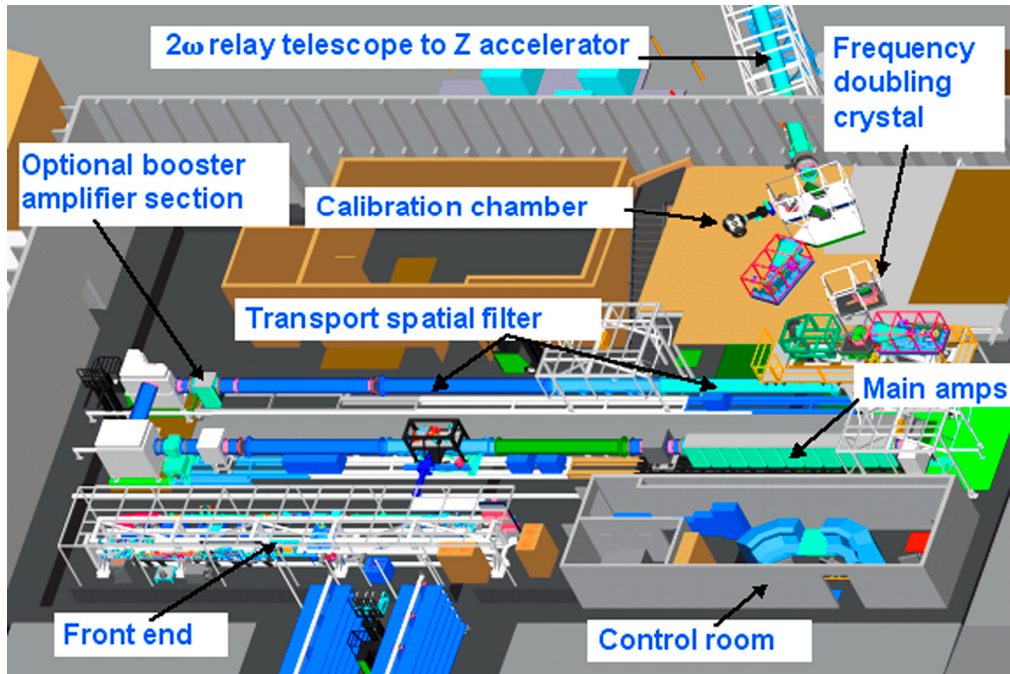


Fig. 2. ZBL layout.

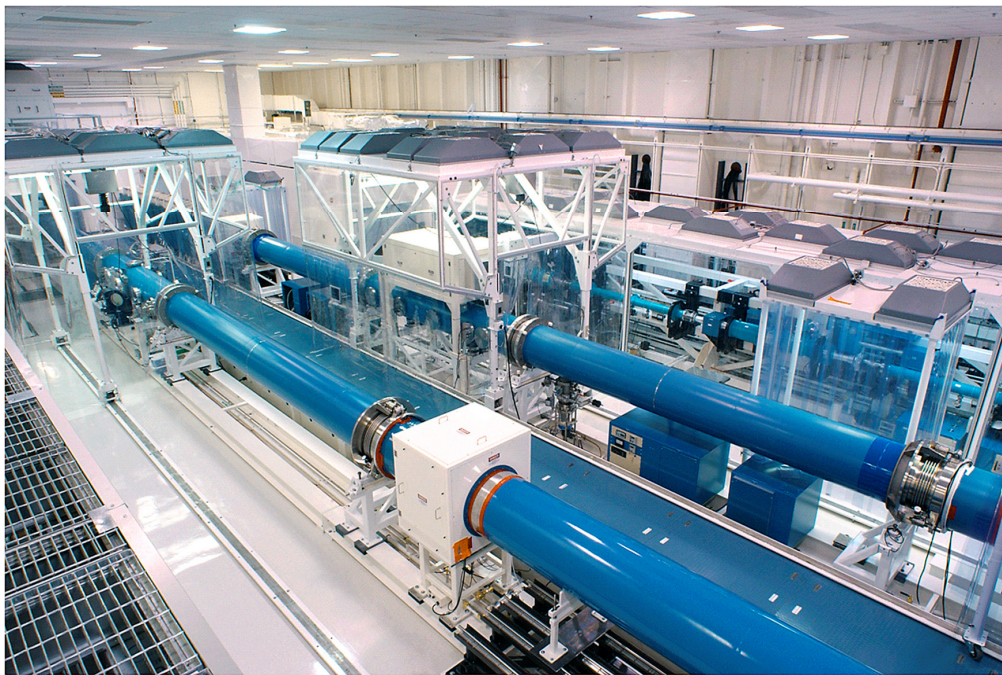


Fig. 3. ZBL Facility.

ZBL was designed to produce > 2 kJ of 2ω energy in up to four pulses of < 2 ns total duration in a 20 ns interval. Through the use of adaptive final optics, it will be possible to focus $> 80\%$ of the 2ω energy onto a single spot or up to four separate spots

of 25–35 μm diameter on a backlighter foil. The resulting irradiances of $4 \times 10^{16} \text{ W/cm}^2$ or greater will make it possible to generate 9-keV x rays from laser-plasma interactions within a thin zinc foil, with adequate efficiency and contrast for backlighting dense objects. ZBL will also be capable of generating x rays over a larger area (1-mm-diameter circle) at lower x-ray energies of 1–3 keV for absorption spectroscopy.

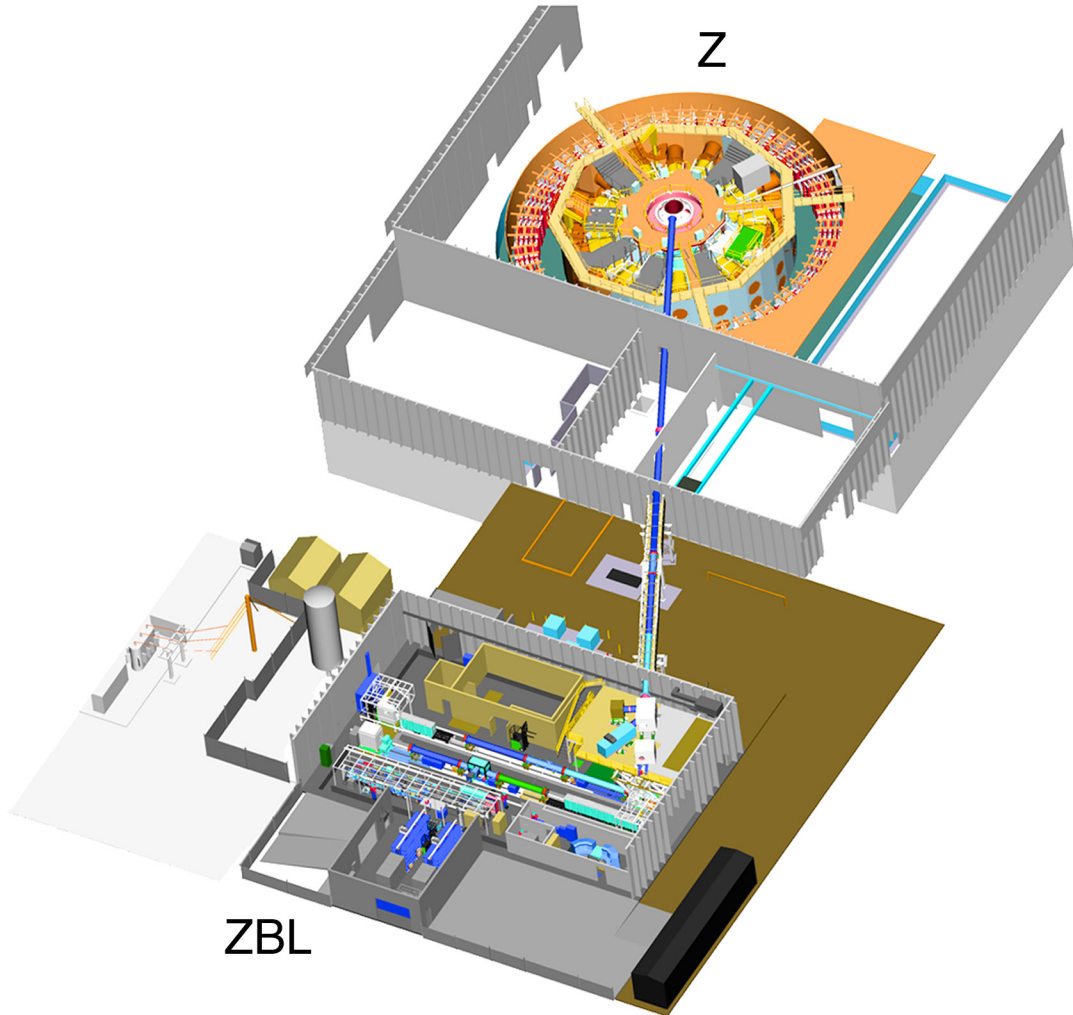


Fig. 4. Layout of ZBL beam transport to the Z machine target chamber.

One primary application for the ZBL system on ZR will be x-ray imaging in the point-projection (PP) backlighting mode (Figs. 5,6), with reduced machine jitter and improved spatial resolution to observe details of capsule implosion experiments at moderate to high convergence ratios. The diagnostic timing jitter for the ZBL system is dominated by the timing synchronization between the laser command fire (from which the ZR machine command fire is derived) and the z-pinch stagnation. Timing jitter of ± 1 ns is a minimally adequate but realistic requirement for single pulse backlighting of transient events, such as fast ignitor capsule compression, taking place in a window of 3 ns or less (see discussion of timing jitter in Sec. IV.10). This requirement represents a

significant improvement over FY02 ZBL synchronization jitter of ± 3 ns. One way to reduce the effects of timing jitter and capture the image of an event occurring in a narrow window with respect to pinch stagnation is to use multiple laser pulses (i.e., up to 4 pulses of less than 500 ps spaced 1 ns apart), focused either on a single spot for a gated imaging detector, or with each pulse focused to a separate spot with a beam-splitter for a non-gated imaging system. The initial goal for multipulse ZBL operation will be a 2-pulse system. Work is in progress to develop a gated, microchannel-plate(MCP)-based imaging detector system for basic point projection imaging on ZR, but there are significant spatial resolution and noise shielding issues to be addressed. In addition to the significant problems of shielding a close-in MCP system in the severe EMP and bremsstrahlung environment of ZR, the spatial resolution achieved using x-ray microscopy may be thrown away using a gated MCP detector in a conventional point-projection backlighting configuration. Our existing gated MCP imaging systems typically have a dynamic range of 100 and a limiting spatial resolution of $> 50 \mu\text{m}$, while film in the detector plane will have a dynamic range of 10^4 and $5 \mu\text{m}$ limiting spatial resolution. (Monochromatic backlighting with 6x magnification coupled to an MCP system can overcome many of these problems.) A 25 mm x 30 mm MCP field-of-view (FOV) would be required to study large diameter capsule implosions. Use of state-of-the-art MCP geometry ($2 \mu\text{m}$ pore size, $3 \mu\text{m}$ center-to-center pore spacing) would provide acceptable spatial resolution.

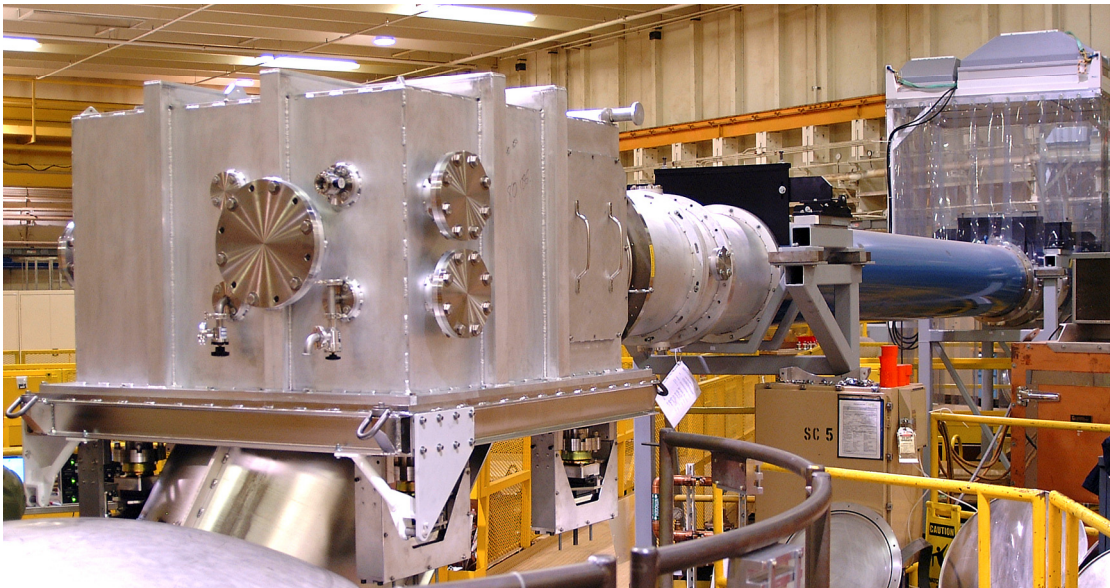


Fig. 5. ZBL beam transport and off-axis FOA (final optics assembly) for high resolution ($\leq 50 \mu\text{m}$) point projection imaging.

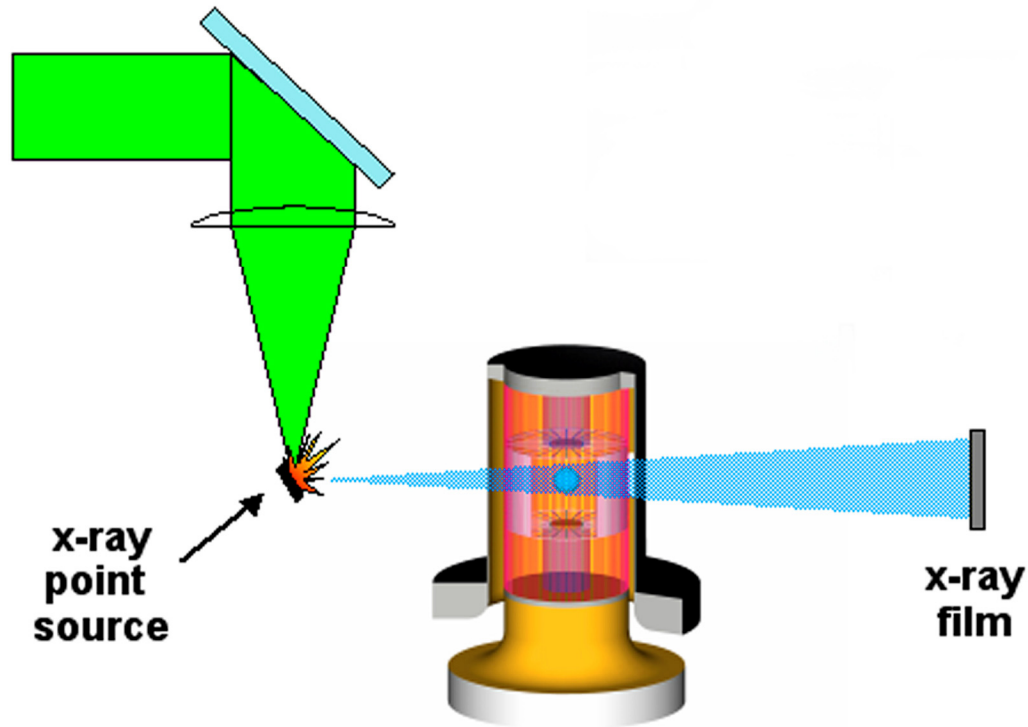


Fig. 6. ZBL point-projection backlighting of capsule in double-ended ZPDH.

The limitations on spatial resolution in point-projection backlighting of 25–50 μm imposed by the size of the laser beam spot and expanding plasma plume on the x-ray source foil may be overcome by using a variety of x-ray optic and microscopy techniques [14-27]. Near-normal crystal microscopy systems have been shown to be more efficient than pinhole camera imaging systems with the same spatial resolution and magnification [14,16]. Also for high-resolution backlighting, bent crystal imaging (BCI) techniques are more efficient than comparable point-projection imaging systems. A curved crystal monochromatic backlighting system is currently being developed on Z for use on ZR [14]. This system can be pre-aligned for insertion as a unit into a ZBL experiment and should provide high spatial resolution ($\leq 10 \mu\text{m}$) with a large field of view and immunity to background noise, but may in practice be limited to an x-ray probe energy of 6.7 keV or less. A complimentary instrument to this would be a Kirkpatrick-Baez grazing incidence microscope which can operate at x-ray energies $\sim 9 \text{ keV}$ for imaging dense plasmas, but has a more complex design and alignment and a limited field of view [5,26,27]. It is recommended that both instruments be developed within an x-ray optics program for ZR, funded at a level of \$500k/year for 6 years. The goal of x-ray optics development should be to create a backlighter imaging system with 5 μm spatial resolution and a 3–5 mm field of view capable of operating at good signal-to-noise levels in the ZR environment. A major differentiating capability on ZR should be the ability to radiate and image large objects with high spatial resolution, providing images with more resolution elements than are presently available at other facilities.

While it would be possible by ZBL beam splitting and use of a second laser beam line and shielded detector to provide orthogonal views of capsule implosions in the horizontal plane, this will not be a very cost effective or space efficient configuration for most experiments. Careful consideration should be given to the possible redundancy of orthogonal views before this complex operating mode is adopted on ZR.

Possible diagnostic applications for ZBL on ZR include:

- (1) High-spatial-resolution PP radiography backlighting (25–50 μm resolution) or BCI radiography (5-10 μm resolution) of ICF implosion capsules in ZPDH [9-11] and DH [12,13] configurations. A side-on backlighting capability with the monochromatic BCI technique may be important for the DH configuration to measure polar symmetry of pellet implosions in secondary hohlraums where spherical convergence is not present. Multiple high-resolution images per shot would be required to study growth of the Rayleigh-Taylor instability in the DH radiation case. Monochromatic BCI is also essential for radiography of fast ignitor capsule implosions because of the need for bremsstrahlung background rejection.
- (2) High-spatial-resolution BCI radiography backlighting for complex hydrodynamics (radjet) experiments to study radiation-induced plasma jetting from structures during radiation transport, as well as for experiments to study more general radiation-induced instabilities.
- (3) High-spatial-resolution PP or BCI radiography of foil expansion in x-ray photoionization experiments.
- (4) High-spatial-resolution PP backlighting as a source for point-projection spectroscopy for pellet implosion and opacity measurements using a close-in, time-integrated spectrometer and collimated point sources sequentially pulsed at multiple locations.
- (5) High-spatial-resolution PP backlighting as a source for double-Bragg-reflection and Laue x-ray diffraction measurements of lattice compression, to determine elastic and plastic strains in polycrystalline and other materials at high pressure using ICE techniques.
- (6) High-spatial-resolution PP backlighting as an x-ray source for transverse measurements of shock and particle velocity in liquid deuterium samples at high pressure. Pressures in this experimental configuration are generated by the impact of a magnetically-driven flyer plate with an aluminum pusher plate in contact with the liquid deuterium sample. Tilt between the flyer plate and the pusher plate forming the front of the liquid deuterium cryocell may be a problem for transverse radiography in a large area, thin cryocell cavity.
- (7) Area backlighting over a 1-mm-diameter circle as a source for absorption spectroscopy and opacity studies. Spatially-resolved absorption spectroscopy could be performed by slit imaging with a large area distributed source.

II.3. Monochromatic Imaging of Z Pinches

A high-spatial-resolution, monochromatic self-emission diagnostic is required to study pinch implosion dynamics, mass distribution, instability growth, and other features of the stagnation of single and nested wire arrays producing up to 350 TW peak power on ZR. Bent crystal imaging techniques can be applied to obtain high resolution images of x-ray self-emission in the 1–6 keV range from a bright x-ray source such as a 20-mm-

long ZR z-pinch plasma [28]. An array of toroidally-bent crystals could be used to obtain gated, two-dimensional images of the z-pinch plasma [29]. Crystal damage from debris and high x-ray flux will be an issue in instrument design. Both chordal and axial lines-of-sight are required for complete characterization of the z-pinch implosion. Modifications of the on-axis diagnostics package will be needed for compatibility with on-axis BCI measurements.

II.4. High Spatial Resolution X-ray Pinhole Cameras

For dynamic hohlraum experiments with single-pinch drive, temperatures are high enough for efficient imaging of pellet implosions by x-ray self-emission. Imploded core x-ray imaging on ZR will require high-magnification, high-spatial-resolution x-ray pinhole cameras [30,31] with sufficient time resolution to image pellet implosions without motion blur. Spatial resolution of 20 μm needed for adequate image detail requires close-in pinholes and higher magnification than currently used to eliminate diffraction limitations on image spatial resolution. It is desirable to have views along and perpendicular to the pinch axis. Orthogonal views will require a reentrant geometry for on-axis observations, with diagnostic pipes intruding into the target chamber from the axial diagnostics package, and in-chamber mounting of a pinhole camera for side-on images of capsules located in a secondary above the z pinch. It may also be possible to obtain side-on images with high energy ZBL point-projection radiography or monochromatic x-ray imaging techniques. Time resolution of 80 ps will be required for imaging of pellet implosions without motion blur, with coverage over a 4 ns window and diagnostic trigger jitter with respect to pinch stagnation of ± 1 ns or less. Use of gated MCPs [32-35] in a close-in geometry will require careful collimation and heavy shielding from bremsstrahlung and EMP background. Debris mitigation will be a particularly difficult problem for on-axis reentrant diagnostics, requiring a combination of imaging apertures (in this case, pinholes), baffles, and fast valves for protection of the imaging plane components.

II.5. Spectroscopy Diagnostics

The spectroscopy diagnostic requirements for ZR experiments must be met by development of instruments with improved spatial, time, and spectral resolution, and by instruments covering a broader spectral range, including UV, VUV, and XUV [36,37], to complement the very effective collection of instruments that have already been developed for visible and x-ray spectroscopy [38,39]. Note that optimized systems can be developed for visible or UV operation, but not both. For example, a UV system could be used in the visible range, but the photocathode response would be compromised. Measurements over shorter time intervals (100 ps) and with higher spatial resolution will require that spectroscopy diagnostics be located closer to the load to maintain an adequate photon flux at the detectors. On the axial diagnostics package [40], compact spectrographs will have to be fielded within reentrant LOS pipes extending into the target chamber. Radial-mounted spectroscopy instruments will need to be located much closer to the load than at present, but not necessarily in a “close-in” configuration on the floor of the target chamber. The availability of radial DIM modules (see Sec. IV.5) would satisfy

many of the requirements for side-on insertable diagnostics packages located near the target chamber wall, below the water level, and needing precise alignment.

At present, a diagnostic access problem exists for radial spectroscopy measurements of DH capsules. It is barely possible to view the capsule side-on with the present 12° LOS. Large-diameter, DIM-compatible 0° lines-of-sight are not a near term option on ZR, and will be considered only as part of a conceptual design for a two-sided z-pinch drive (see Sec. IV.19). Raising the load sufficiently to completely eliminate this problem imposes a severe inductance penalty on pinch power and hohlraum temperature. Reconfiguring the MITLs to raise the source position is also not an option being considered for ZR. It appears that a combination of raising the source slightly and careful redesign of the pinch glide plane is the only solution to this spectroscopy diagnostic access problem.

Trigger jitter is a critical issue for improved time resolution for spectroscopy diagnostics. While it may be possible to reduce timing jitter from command fire to pinch stagnation to the level of ± 1 ns (see Sec. IV.10), diagnostic triggers with ≤ 500 ps jitter to meet the timing requirements for faster framing cameras would need a more precise trigger derived from some forward point such as a load B-dot. Low-jitter trigger sources for diagnostics requiring a minimum of trigger delay with respect to pinch stagnation should be investigated as part of spectroscopy as well as imaging diagnostic development.

A number of specific recommendations can be made for development of new spectroscopy instruments. For EOS studies [41,42], the present visible spectroscopy instruments should be replaced with multiple fiber-optic-coupled UV instruments. It would also be useful to field a deep UV instrument with improved time resolution lens-coupled through an open relay path. Appropriate enhancements in ZR infrastructure will be required to provide the necessary relay paths. A high spectral resolution visible system should be implemented in addition to the survey instruments normally used for EOS temperature measurements. Such an instrument could be useful for measuring the distribution of velocities in a shock front, as well as providing capability for z-pinch and powerflow measurements. It could also serve as the detector system for a Thomson scattering diagnostic (Sec. II.6.). EOS studies require highly accurate calibrations. This capability would be enhanced in the visible region by converting to CCD recording of the streak camera output. UV systems will also be of little value for EOS studies without the development of accurate absolute calibration equipment and procedures. For opacity measurements, the capability should be developed for fielding cross-calibrated, time-resolved x-ray spectrometers on two different lines-of-sight. An in-chamber, high sensitivity elliptical crystal spectrometer should be developed for high spatial resolution ICF capsule measurements, for opacity studies of heavily tamped samples that transmit only a small fraction of x-rays, for accurate recombination continuum measurements of photoionized plasmas, and for space-resolved absorption spectroscopy using ZBL. Such an instrument is scheduled for deployment on Z in FY03. ZR infrastructure must be designed to accommodate an instrument of this type. Fast and reliable instrument alignment will be facilitated by the availability of a center-section test stand (Sec. IV.16). The flexibility to field multiple copies of core x-ray spectroscopy instruments on up to four different lines-of-sight should be developed for studies of z-pinch emission uniformity.

II.6. Thomson Scattering Diagnostic

A time- and space-resolved Thomson scattering diagnostic should be implemented as a high priority. Capabilities of this instrument should include multi-point measurements of: (1) z-pinch implosion velocity, spatial velocity distributions, and temperature; (2) primary and secondary filling, including electron temperature and density measurements; and (3) temperature and density of radiation-heated samples, including foils, foams, and gas cells. System features should include tripling or quadrupling a portion of the ZBL beam, an open beam line for lens-coupled insertion of the beam, rapid alignment of collection optic systems, and a high-resolution, time-resolved spectroscopy detection system.

II.7. Extended Range Soft X-ray Spectrometer

It is recommended that a soft x-ray spectral diagnostic be developed to measure pinch and hohlraum wall temperatures over a wider range than is presently possible. This could be an instrument similar to the present Transmission Grating Spectrometer (TGS) [43], but with additional silicon p-i-n diodes, operated with multiple sensitivities to cover brightness temperatures from 50 to 300 eV. Such an instrument would make it possible to study the spectral evolution of a single x-ray emission area during both the z-pinch implosion and stagnation phases.

II.8. Hard X-ray Spectrometer

Plasma instabilities can generate on-axis electron beams during pinch stagnation and thermalization [44]. Hard x-rays (>10 keV) resulting from the interaction of these electron beams with surrounding pinch and hohlraum material (as well as the hot electrons themselves) may preheat the fuel pellet, particularly in dynamic hohlraum configurations. Existing z-pinch characterization diagnostics provide coverage of the x-ray energy range from about 100 eV to 10 keV. Diagnostics with adequate time and spatial resolution for measuring energy and temperature of the hard x-ray radiation are required on ZR to determine the effect of on-axis electrons on target preheat and to assess the hard x-ray background from the pulsed radiation source for weapons effects experiments.

An in-chamber hard x-ray spectrometer with a range of 10–100 keV is currently being developed [45] for ZR by Special Technologies Laboratory, a division of Bechtel-Nevada. The spectrometer body consists of a heavily shielded steel collimator providing a spatially localized view of the target with a 1-cm-diameter circular field of view for each of six discrete channels. Techniques to be utilized for obtaining spectral cuts of the hard x rays include filter absorbers, Ross filter pairs, and filter fluorescers. Silicon photodiodes with time response of 1 ns make up the detector array of 6 discrete filtered channels and one background channel whose signals will be recorded on 3 GHz digitizers for unfold of the high energy spectrum. Initial testing of this instrument has begun on ZPDH shots on Z.

II.9. Neutron Diagnostics

Neutron diagnostics provide essential information on the state of the compressed fuel core in an ICF target [46,47]. The type and accuracy of neutron measurements that are possible for a given experiment depend on the total thermonuclear neutron yield from the target. An initial requirement for diagnosing fuel capsule implosions on ZR in the ZPDH double-pinch geometry is a total neutron yield detector system with a 5×10^6 neutron detection threshold. Neutron total yield diagnostics based on nuclear activation [48,49] have a measurable range only down to about 5×10^8 neutrons for accurate measurements. In a different approach, a high sensitivity neutron yield detector is currently being developed with massive stainless steel and tungsten shielding extending in to the load can (Fig. 7). The detector is collimated to view only the imploding fuel capsule in a ZPDH double-pinch geometry, where the capsule is in a secondary hohlraum separated from bremsstrahlung sources associated with the pinches in the two primary hohlraums. In the DH configuration, the fuel capsule is contained within the pinch or just above the pinch, and this collimation would not be effective. The collimated channel in the shielding fans out to a large solid angle scintillator (10 cm L x 2.5 cm W x 2.5 cm thick) and PM tube detector with time response of a few ns, located about 1 m from the source. Based on preliminary measurements of bremsstrahlung flux from the load and feed region, sufficient shielding is provided to reduce the bremsstrahlung reaching the detector to a level below the energy deposited by 5×10^6 neutrons. Testing of this high sensitivity neutron yield diagnostic will begin in FY03 to evaluate the effects of severe scattering of MeV photons within the shield that could illuminate the scintillator and distort the neutron signal.

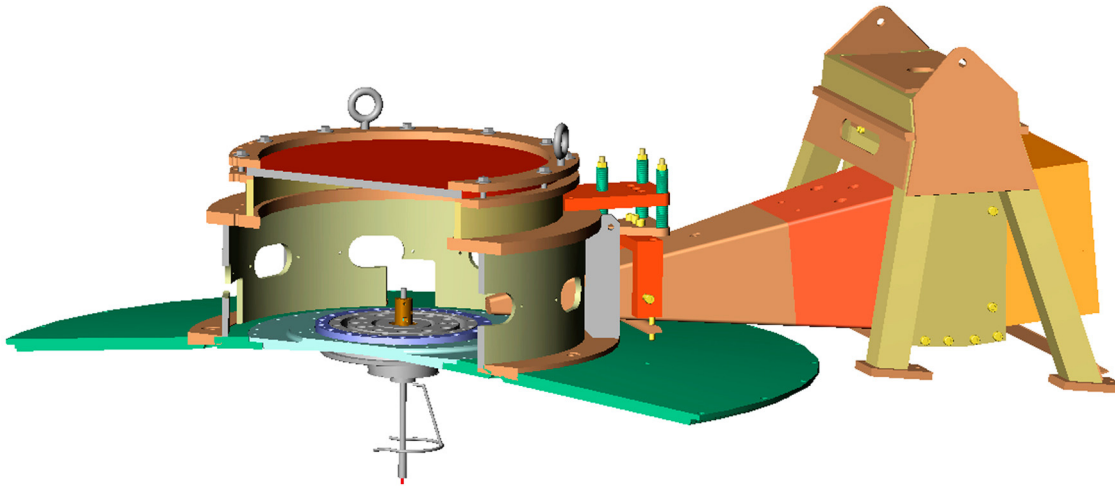


Fig. 7. In-chamber, shielded low threshold neutron yield detector (under development).

A second basic neutron diagnostic required for initial fuel capsule implosion experiments on ZR is a neutron time-of-flight (TOF) detector system [46,47,50,51]. Neutron TOF measurements of the energy broadening of DD and DT neutrons can determine both the neutron total yield and the fusion burn ion temperature. Such measurements become practical for DD reactions at neutron yield levels of $10^8 - 10^{10}$, a range that has recently been achieved on Z in the high temperature DH configuration. Neutron yields for DT reactions on ZR should be two orders of magnitude higher, in the

$10^{10} - 10^{12}$ range, for comparable sized targets. LOS requirements for a neutron TOF detector system are determined by the reactions of interest and by the need to distinguish between thermonuclear neutrons from a fusion burn and beam-generated neutrons. The neutron energy half-width, which is related to burn temperature, can be extracted from the TOF distribution of neutrons arriving at the detector. The flight path of the neutrons must be long enough to produce a pulse whose width can be accurately measured. Also, the TOF spread of the higher energy DT neutrons is significantly less than for DD neutrons, requiring a longer flight path for DT neutrons to obtain comparable resolution. Beam-generated neutrons tend to be higher in energy than thermonuclear neutrons and to have an anisotropic distribution peaked in the direction of the beam. Beam-generated neutrons can be distinguished from neutrons of thermonuclear origin by the arrival time of the neutron pulse and by the angular distribution of the neutron fluence.

The requirements for accurate neutron TOF measurements represent a significant challenge at lower DD neutron yield levels of $1-5 \times 10^8$ neutrons that might be encountered in ZPDH double-ended hohlraum capsule implosion experiments. A flight path sufficiently long to provide a measurable pulse width may not yield statistics adequate to accurately define the pulse shape. Inadequate statistics can be overcome through the use of very thick scintillators (~ 25 cm), but the added neutron transit time can also distort the neutron profile. Forward-going neutrons from beam-generated phenomena are generally very broad in energy and can interfere with the thermonuclear component of the neutron time profile, while beam-generated neutrons emitted at 95° to 105° from the z-pinch axis can have a significant component close to the 2.45 MeV DD reaction peak. The anisotropy test to distinguish thermonuclear from beam-generated neutrons requires detectors along the z-pinch axis. In the ZPDH configuration, the detector FOV will now include the two z pinches on-axis as well as the capsule, and a heavily-shielded collimation system will not be effective.

At present, two heavily-shielded neutron TOF detectors collimated to look at the source region are located about 8 m from the source, at 12° above the horizontal plane on radial LOS 25/26 (Fig. 8) and on-axis in the basement. To meet experimental requirements on ZR, four neutron LOS pipes will be required, two on-axis above and below the pinch, and two at 12° above the horizontal plane, 180° apart azimuthally. Minimum requirements to be included in the initial ZR design should be two neutron LOS pipes, one on-axis, directly below the pinch in the basement, and one side-on LOS at 12° . A long (50–100 m) LOS for neutron measurements at 12° would require the construction of a tower outside of the ZR building to access detectors. Whatever the configuration of LOS pipes, it is imperative that each LOS have two or more neutron TOF detectors at known separation. By measuring two neutron signals on the same LOS, the energy and production time of the emitted neutrons can be accurately determined.

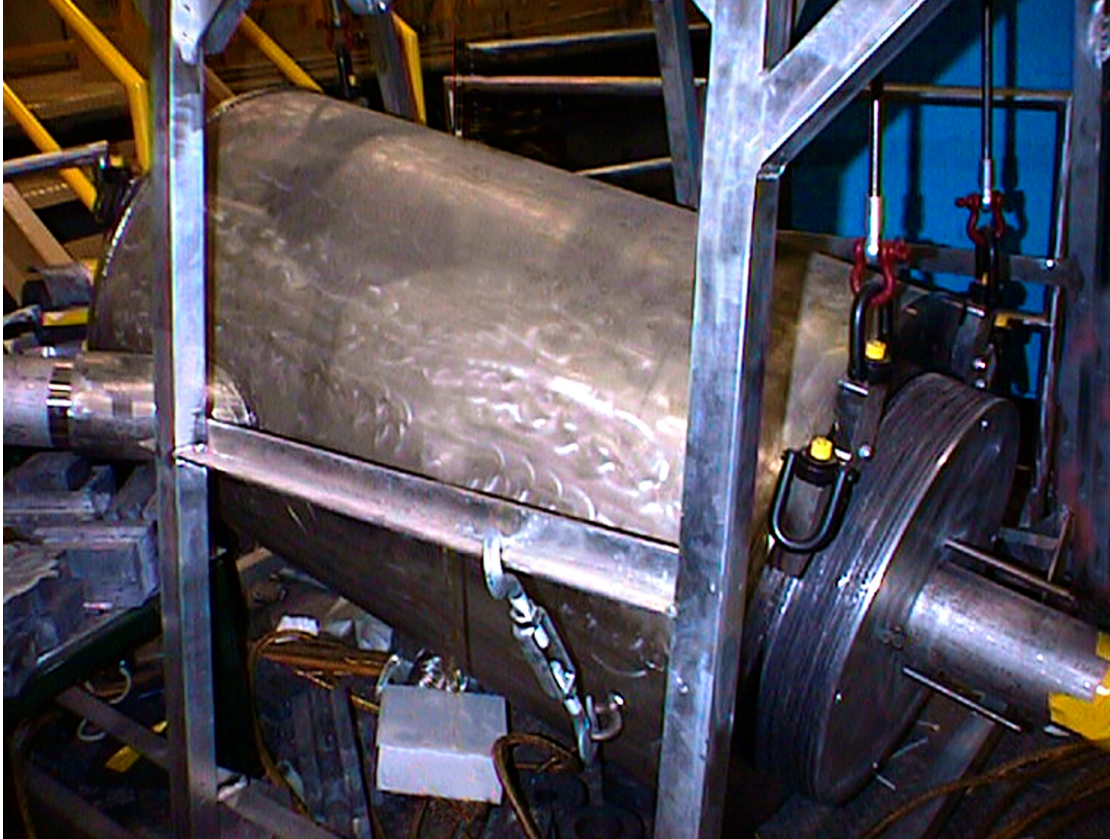


Fig. 8. Neutron time-of-flight diagnostic in 900 pound shield on LOS 25/26.

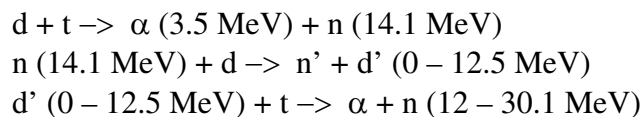
The intense bremsstrahlung background environment on ZR can be countered at higher neutron yield levels through precise collimation and alignment of shielded detectors, by TOF separation of neutrons and bremsstrahlung over a long flight path, and by the use of gated detectors. For non-gated TOF detectors, it is necessary to avoid saturation by the bremsstrahlung pulse or to allow sufficient time for recovery from saturation to a steady state before the neutron arrival time by the use of long LOS pipes. Shielding requirements can be reduced by using relatively compact neutron detectors consisting of fast plastic scintillators coupled through a MCP to a photomultiplier tube.

The time history of target thermonuclear emission and the time to peak thermonuclear emission (target bang time) are quantities that depend strongly on the details of target hydrodynamics and plasma conditions and provide a sensitive test for simulations of target behavior [46,47,52,53]. Fusion reaction history diagnostics become practical for neutron yields of $10^{10} - 10^{12}$. Burn history measurements were routinely performed on Nova with fast detectors located close to the target. Gamma-ray methods are being investigated for use on NIF, where larger separation distances (5 m) are required for survivability of the instruments. These techniques require fast, sensitive gamma-ray detectors that would need careful shielding and precise collimation in the ZR bremsstrahlung environment. By proper modeling of the responses of multiple neutron TOF detectors on the same LOS, it may be possible to unfold the target burn history and bang time. Three detectors on each neutron LOS may be required to accomplish this measurement. A range of possible techniques should be investigated to develop a target

burn history diagnostic with 20 ps resolution and a bang time diagnostic with 50 ps resolution suitable for use in the bremsstrahlung environment of ZR.

Measurements of fuel areal density $\langle \rho r \rangle$ are essential for characterizing ICF target capsule implosions and are traditionally performed using a number of neutron-based techniques [46,54-56]. One method involves the detection of secondary neutrons produced in reactions in pure deuterium fuel and is useful for $\langle \rho r \rangle$ values below about 20 mg/cm² [57]. Since experiments with DD fuel will be the first step in ICF fuel pellet implosion studies on Z and ZR because they produce a minimum of nuclear contamination in the center section and permit high shot rates, measurement of secondary neutrons is an excellent technique for initial $\langle \rho r \rangle$ studies on ZR. In this method, the product triton from the primary reaction $d + d \rightarrow p + t$ (1.01 MeV) produces a secondary reaction with the fuel deuterons $d + t \rightarrow \alpha + n$, producing neutrons with energies between 11.8 and 17 MeV. The triton fraction that undergoes this secondary reaction is directly proportional to the fuel $\langle \rho r \rangle$ for values of fuel areal density < 20 mg/cm² where there is no significant slowing of the triton in the fuel and the secondary reaction cross section remains approximately constant. Areal density can be determined by measuring the ratio of secondary reaction neutrons to primary neutrons from the other DD reaction branch $d + d \rightarrow n + {}^3\text{He}$. A neutron spectrometer should be developed for ZR with better than 100 keV resolution and 10⁶ neutron detection threshold for secondary neutron $\langle \rho r \rangle$ measurements and also for fuel ion temperature measurements.

For $\langle \rho r \rangle$ values larger than about 20 mg/cm², tertiary neutrons produced in the DT reaction chain



can be used to measure fuel $\langle \rho r \rangle$ [40]. For areal fuel densities to > 1 g/cm², the number of tertiary neutrons produced is proportional to $\langle \rho r \rangle^2$. An angular distribution of tertiary neutrons with energy > 28 MeV obtained from an array of neutron detectors can provide direction information on $\langle \rho r \rangle$. A tertiary neutron detector system with a 40 m flight path is being developed for NIF.

For yields of $> 10^{12}$ neutrons from large DT targets on ZR, neutron core imaging becomes possible. This method is almost completely insensitive to target areal density at the point where x-ray imaging techniques fail because of photon absorption [46,58-60]. High spatial resolution and good sensitivity can be achieved using penumbral or annular coded aperture techniques similar to those that were employed in the Nova neutron microscope [61]. A close-in diagnostic with a high-efficiency, low resolution detector operating at high magnification can produce images with 10 μm resolution over a limited field of view of 300 μm . A neutron imaging system should be developed for ZR with a spatial resolution of < 50 μm and a 500–1000 μm field of view. The thick neutron aperture on the collimation system can provide shielding and survivability for the instrument detector system in the ZR blast environment without the requirement for a fast closing shutter, but precise laser alignment of the aperture is required because of the limited field of view.

II.10. VISAR System Development

Shock physics experiments on ZR [41,42,62,63] in support of the Dynamic Materials Properties Campaign (C2) will take advantage of the higher currents (28-30 MA into an ICE short circuit panel load) and the enhanced current pulse shaping capabilities of ZR to extend ICE and EOS measurements to higher pressures and new materials. New VISAR [58] instrumentation will be required to support these shock physics experiments. At present, there are 8 Sandia-owned and 28 Bechtel-Nevada-owned single-point VISARs in use on Z experiments. There is a need for more Sandia-owned VISARs to increase the overall number of VISAR channels available for experiments on ZR and to ensure the continuous availability of a core group of VISARs for use when the BN instruments are deployed elsewhere. An additional group of 14 SNLA-owned VISAR channels should be purchased in FY03 for about \$400k.

There is a need to improve the velocity accuracy of the VISARs to optimize data quality for dynamic materials properties studies. The time resolution of single-point VISARs can be improved from about 1 ns to 100 ps. Modifications to the line-imaging VISAR can improve the time resolution from 50 ps to 1 ps. It would be desirable to develop a second line-imaging VISAR for ZR (which could also be shared with experiments on Saturn) to study 1-D drive uniformity and Rayleigh-Taylor instabilities for multiple magnetically-driven foils on a single experiment. There is also a need for a full-field, gated multiframe VISAR interferometer to measure time-resolved 2-D drive uniformity over an entire target area. A new fast framing camera has been acquired for this purpose. The addition of a second open-beam optical port on the target chamber with access to the LOS 9/10 screen room will be required to accommodate line and full-field VISAR development on ZR.

II.11. Imaging Shock Breakout Diagnostic

There is a need for an imaging shock breakout diagnostic to aid in interpretation of data from fiber-optic-coupled active shock breakout (ASBO) and passive shock breakout (SBO) single-point probe arrays [39,46]. Line VISAR imaging of a 1-D region on an identical target is a ideal way to perform this measurement. Direct optical imaging of a slit-defined 1-D region through an open beam optical train onto a streak camera is another possible option. This application reinforces the need for at least two open beam optical trains in the center section with periscope turning mirrors, access to a nearby dedicated screenroom, and adequate streak camera support.

II.12. Laser Plasma Probes

Laser diagnostics are currently being developed on Z as a sensitive probe to characterize low density plasmas encountered in the early phase of z-pinch implosions and target illumination. Mechanisms that are being explored for imaging the plasma distribution with laser probes include refraction of the probe beam (interferometric, Schlieren, and shadowgraphic imaging), reflection of the probe beam from the critical density front, absorption of the probe beam, and inverse bremsstrahlung absorption [65,66]. There are a wide range of potential applications of these laser probe techniques

to z-pinch-related physics problems, including the study of wire initiation and implosion dynamics, current density distribution during implosion, foil ablation, plasma distribution on-axis and around apertures in the dynamic hohlraum configuration, plasma streaming and jetting, and gas cell ionization rates. A variety of CW, long pulse, and short pulse lasers are being employed in Z laser probe experiments, with open beam and fiber optic delivery of light to the target chamber and streak and framing camera data recording in the LOS 9/10 screenbox. Extensive shielding and baffling of the image region near the load is required to overcome self-emission from the z-pinch.

The power of these laser probe techniques was demonstrated in an initial study of plasma density and velocity during x-ray-generated foil expansion. The large field of view required for these measurements could be applied to the study of precursor plasma evolution in a dynamic hohlraum. A streaked chordal laser probe is also being developed for wire run-in plasma studies. The effects of wire expansion and jetting during wire array implosions have been observed in these measurements. The continued development of laser probe diagnostics should be vigorously supported through the acquisition of required lasers, streak cameras, and framing cameras, and through a limited number of dedicated diagnostic development shots if appropriate.

II.13. Pulsed Power Flash Radiography System

Using the magnetic pressure generated in high current density geometries on ZR, it is anticipated that magnetically-driven flyer plates for EOS measurements can be accelerated to velocities approaching 40 km/s, much higher than are possible in traditional gas gun experiments. There is a need for a pulsed power radiography system on ZR to be used as a flash x-ray source to measure the integrity of magnetically-driven flyer plates. Other applications might include the observation of motion in small structures irradiated with z-pinch x rays for weapons effects studies.

II.14. Visible Imaging Hydrotest Capability

It would be desirable to have the ability on ZR to image physics experiments using transport optics, a structured light grid projection capability, and a visible framing camera. This hydrotest capability would provide information about the surface motion and distortion of structures mounted on the primary hohlraum and would be of value for weapon physics experiments in combination with other diagnostic techniques such as backlighter x-ray imaging. The beam-turning periscope, open-beam optical port, and fast framing camera required for the full-field multiframe VISAR system under development for ZR could also serve as basic components for a visible imaging hydrotest system.

III. Improvements to Existing Diagnostics for ZR

III.1. Introduction

Many of the diagnostics required to measure pinch power and energy, hohlraum wall temperature, aperture closure, x-ray spectra, shock pressure, and other essential parameters for weapons physics, ICF, HEDP, and dynamic material properties studies have already been developed over the last 20 years for use on Z and will form the core of diagnostics packages to be fielded on ZR. Diagnostics currently in use on Z are described briefly in Appendices A1-A5 and in more detail in Refs. 39,40. A program to continuously improve the range, operation, reliability, calibration, alignment, data quality, and other essential features of these core diagnostics is presently underway independent of the ZR Project.

This section will describe some of the major improvements to existing Z core diagnostics that are currently in progress, or that are required in the future for measurements on ZR. A major advance for many existing core diagnostics would be the ability to field multiple copies of that diagnostic at several different positions on a single shot, with some flexibility in the choice of diagnostic location. This requirement cannot generally be met at present on Z, and will be satisfied only through the ZR diagnostics infrastructure improvements described in Sec. IV.

III.2. Upgrade of the LOS 5/6 Diagnostics Package

Z-pinch x-ray power production is the ultimate test of power flow to the load region. An ongoing effort to improve power flow diagnostics is presently focused on z-pinch power diagnostics on radial LOS 5/6 [39]. This is the longest LOS pipe complex on Z (Fig. 9), with one LOS pipe section extending to 26 m. The LOS 5/6 diagnostics package is designed to provide the primary x-ray energy, power, and spectral measurements of the z-pinch itself. Five port locations exist and are typically used to field instruments including a bolometer array [67], an x-ray diode (XRD) array [68], a photoconducting detector (PCD) array [69-71], a transmission grating spectrometer (TGS) [43] (Fig. 10), and a total energy and power (TEP) diagnostic [72] or a calorimeter [73]. As part of the overall LOS 5/6 diagnostic upgrade, improved mounting fixtures for the diagnostic LOS pipes have been installed to provide for more rapid, accurate alignment of the z-pinch x-ray power diagnostics.

Incremental changes are being made in the resistive bolometer design and operation to improve the accuracy of x-ray energy measurements out to 1.5 keV and to reduce signal noise to allow the direct extraction of accurate x-ray power waveforms by differentiation of the bolometer energy waveforms. Techniques for the fabrication of nickel bolometer resistance elements are being continuously improved. Better digitizers with reduced bit noise and greater offset result in recorded bolometer signals with improved dynamic range and significantly reduced noise. A 3-bolometer array containing both old and new bolometer elements has produced total energy measurements consistent to within a few percent. These steps should greatly improve the

absolute accuracy of the standard procedure for obtaining a pinch power waveform, which has been to normalize the integral of the XRD Kimfoil channel (250 eV) signal to the bolometer energy measurement. Discrete noise spikes on the radial LOS bolometer signals are probably the result of inadequately suppressed photoelectron emission from the bolometer resistance element. Solving this problem with higher transverse B fields will make it possible to differentiate bolometer energy signals to obtain accurate power waveforms [74].

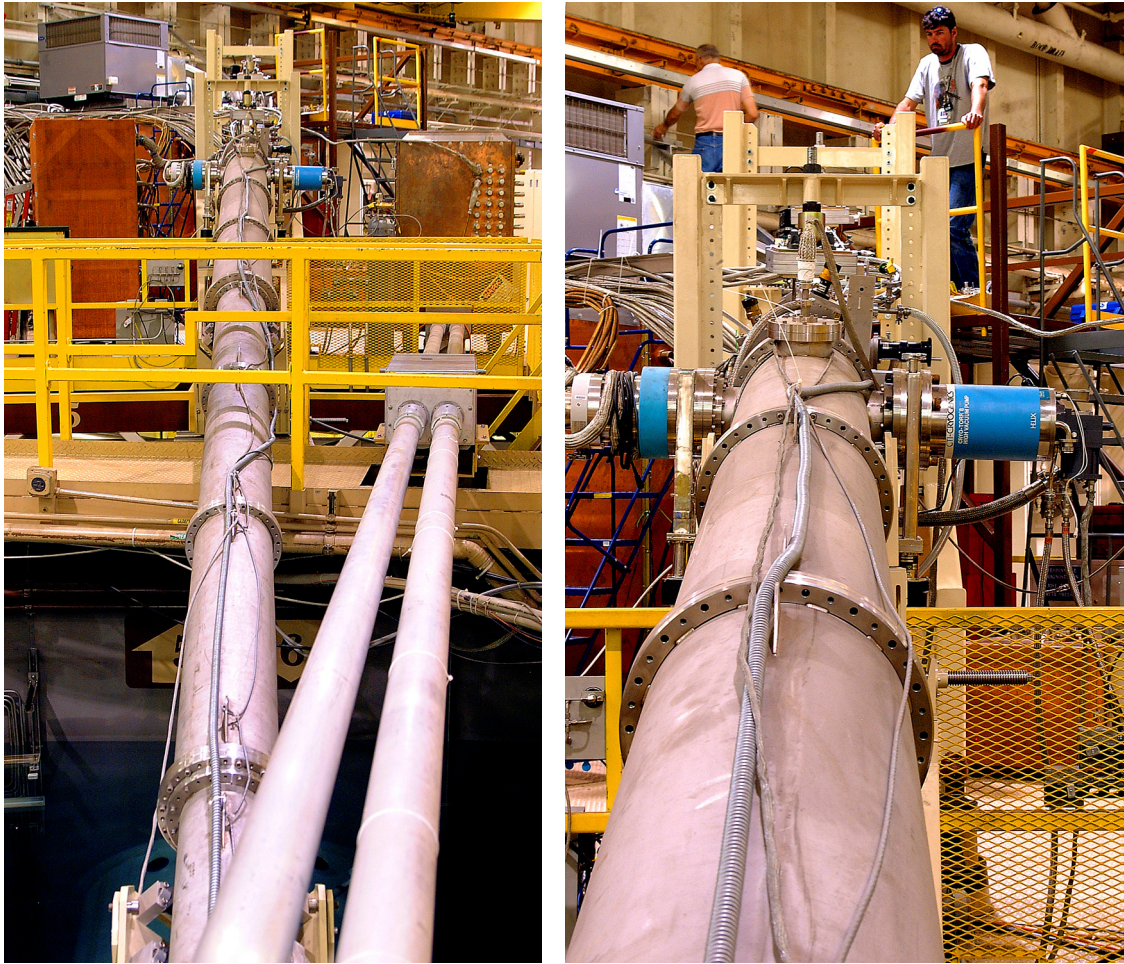


Fig. 9. LOS pipe and vacuum system for LOS 5/6 diagnostics.

A filtered 6-channel PCD array covering the x-ray energy range from 1–6 keV is currently fielded at 19 m on LOS 5/6. The PCD array is used to estimate the slope of the free-bound continuum for z-pinch emission and to derive the pinch electron temperature as a function of time. It is recommended that the PCD array spectral response be extended to 10 keV through the addition of higher energy channels. At present in dynamic hohlraum experiments, it is impossible to distinguish between a non-Planckian spectrum of x-ray emission resulting from a nonthermal component of hot electrons and a spectrum consisting of two Planckian components, with one of the components coming

from a very hot core. By extending the PCD spectral response and performing absolute PCD calibrations, this question might be resolved.

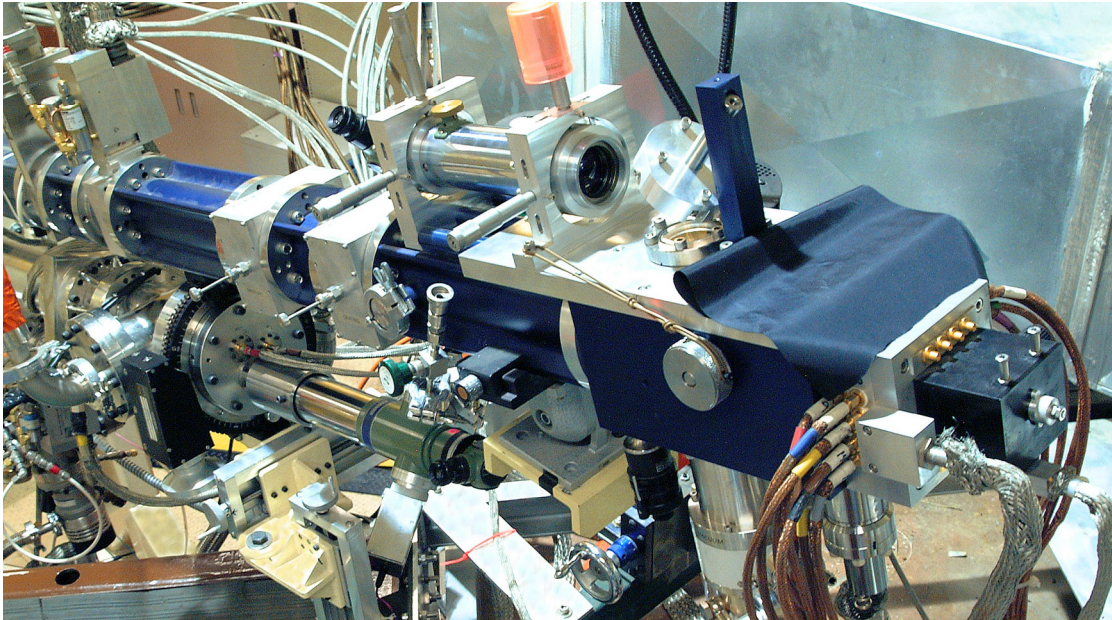


Fig. 10. Transmission grating spectrometer and alignment telescope on LOS 5/6.

A new x-ray power diagnostic called TEP [72] is being developed on LOS 5/6 to cover the spectral range from 100 eV to 4 keV. Mounting hardware has been designed to make the TEP interchangeable with the calorimeter x-ray energy diagnostic which is preferred by some users. The TEP detector package consists of four pinhole-apertured silicon diodes and an alignment telescope mounted behind a standard 5-channel fast valve to prevent debris damage to the aperture plates. Pinhole imaging reduces incident flux by a factor of 3000, so that this diagnostic can operate up to the maximum x-ray peak power level of 350 TW expected on ZR without an LOS pipe extension.

It would be highly desirable to field multiple copies of these improved diagnostics on other radial lines-of-sight to characterize the spatial distribution of z-pinch radiation. The ability to do this is very limited on Z and a prime objective of infrastructure development for ZR.

III.3. Improved Load Current Monitors

As part of the effort to develop improved power flow diagnostics [75], a new load current monitor is being tested on Z for use on ZR [76]. This diagnostic consists of an array of eight calibrated B-dot monitors at the bottom of a magnetically-insulated azimuthal anode groove of L-shaped cross section located at the minimum radius where flashover will not occur. This arrangement serves to smooth the current distribution, shield the B-dots from direct electron strikes, and provide a statistical average over many measurements in a symmetrical geometry. This design should result in current measurements accurate to a few percent for currents up to 28 MA and will be the new

standard current diagnostic close to the load. The design of individual calibrated B-dots operating at the anode surface is also being continuously improved to provide a range of options for current measurement where a full grooved array of B-dots cannot be accommodated.

III.4. Large Format Framing Camera

A large format (70 mm film) time-resolved x-ray framing pinhole camera is mounted on LOS 9/10 for detailed imaging of the full-length z-pinch implosion and stagnation [39]. The detector array consists of nine 2 cm x 3 cm MCPs, each gated with a 100-ps-wide pulse. This provides adequate time resolution to avoid motional blurring up to pinch velocities of 1×10^8 cm/s. The present pinhole camera spatial resolution is 75 μm at a magnification of 1.7.

To track the time history of Rayleigh-Taylor instability development in z-pinch and the trajectory of pellet implosions for dynamic hohlraum experiments in more complete detail, it is necessary to record many more frames during the event sequence while improving the overall reliability of the camera system. This can be done by increasing the camera magnification from 1.7 to 5 and projecting four separate target images on each MCP, using the TOF of the bias voltage pulse across the MCP to provide the required time resolution. In this arrangement, up to 36 sequential images can be obtained with 70 ps time resolution with a 4-mm-wide by 3-mm-high field of view. Because of the large number of frames and relatively wide event window possible with this diagnostic, diagnostic timing jitter with respect to pinch stagnation of ± 1 ns would be quite adequate to capture the details of a transient event such as pinch stagnation.

III.5. Active Shock Breakout (ASBO) Diagnostic

There is a need to upgrade the 1-D spatially-resolved fiber-optic-coupled active shock breakout (ASBO) imaging system used on dynamic hohlraum experiments. An improved fiber transport array is required, with green laser light to match the streak camera photocathode sensitivity and 100 μm spatial resolution over a 15 mm field of view with 50 ps time resolution. A second full imaging transport system for a second target would also be valuable. Several visible streak cameras, possibly facility owned and shared among users in the LOS 9/10 screenroom, will be required to record fiber-optic-coupled single point and line-resolved ASBO data. Some existing streak cameras are dying and will need replacement.

III.6. Time-resolved X-ray Crystal Spectrometer

A 1–10 keV time-resolved x-ray crystal spectrometer is being developed by Bechtel-Nevada for use on LOS 21/22. This instrument uses two dispersive crystals, each with 10 silicon photodiodes, as spectral detectors with better than 1 ns time resolution. This instrument was calibrated at Brookhaven National Laboratory in FY02, in preparation for testing at the University of Nevada Reno on Nevada Terawatt Facility High Current X-pinch experiments before fielding on Z. A duplicate of this instrument might eventually be included as part of the LOS 5/6 diagnostic package. The availability

of sufficient fast digitizers is an issue for fielding multiple copies of this diagnostic on ZR.

III.7. Replacement of Standard Convex Crystal Spectrometers with Elliptical Analyzers

At present, four convex crystal x-ray spectrometers can be fielded on radial LOS 13/14 at 12° , covering a range of 1-10 keV with spectral resolution of about 500 limited by source broadening [39]. The two time-integrated KAP convex cylindrical crystal spectrometers with slit-defined 1-D spatial resolution of 100 μm to 1 mm and a film-based detector system have adequate sensitivity for absorption spectroscopy measurements on Z and are valued for their highly reliability. The two time-resolved, spatially-integrated KAP spectrometers, with 7 frames, 1–2 ns gates, and a more limited spectral range because of the 4 cm length of the MCP, will be replaced over the next two years with more advanced elliptical crystal spectrometers [77] which feature higher sensitivity and much better signal-to-noise levels. The time-integrated convex crystal spectrometers will be retained. A double elliptical crystal spectrometer, a single instrument with two crystals and detector systems, is also being developed for use on LOS 33/34.

The capability should be developed to field time- and space-resolved elliptical crystal spectrometers on 3 separate radial lines of sight along with 3 time-integrated instruments. Streak camera detection systems should be available to augment framing camera systems. Mounting hardware should be developed to allow convex crystal and elliptical geometry instruments to be easily and reliably interchanged, depending on the experiment.

III.8. Additional TREX Instruments

The TREX instrument is a time-resolved crystal x-ray spectrometer [78] with 1-D slit-defined spatial resolution and a detector system presently consisting of an MCP and 6-frame camera. It is used to measure the capsule implosion x-ray spectrum on dynamic hohlraum experiments. Axial measurements of time- and space-resolved argon emission lines from deuterium capsule implosions with argon seed gas can be used to determine electron temperature and density and to infer implosion symmetry. Additional TREX instruments are currently being developed for radially- and axially-resolved side-on (12°) measurements of polar implosion symmetry and max-min capsule convergence for dynamic hohlraum pellet implosions.

III.9. Calibrated Streak Camera Systems

There is a need for calibrated optical streak camera systems [79-86] for use with the EST (Energy, Space, and Time) 1-D imaging system and with slit-imaged time-resolved spectroscopy systems for accurate quantitative measurements of axially-resolved pinch emissions, temperature, and other parameters. It is recommended that several new streak cameras with stable, reliable performance be acquired over the next six years and

that the performance of all active streak cameras be checked periodically against specifications by Bechtel-Nevada to verify sweep linearity, system sensitivity, spatial resolution, and other relevant parameters. As a general principle, there should be a transition to streaked spectroscopy for survey spectroscopy instruments used in the study of z-pinch physics.

III.10. Improved Diagnostic Request Form

A user-friendly Web-based diagnostic request form is being developed with sufficient detail to completely and unambiguously specify a diagnostic shot setup.

IV. Diagnostic Infrastructure and Operational Issues for ZR

IV.1. Introduction

One of the primary criteria for the ZR Project [2] is to “provide standardized access and supporting infrastructure for diagnostics”. The present diagnostics infrastructure on Z has in many respects evolved independently for each group of diagnostics to the extent that there is little flexibility in the location of individual instruments and no available access for new or temporary diagnostics. A systems level approach to diagnostic support on ZR should significantly improve diagnostic access and flexibility, while providing for the efficient and reliable operation of diagnostics that will allow the ZR facility to support a 400-shot-per-year program.

This section discusses a number of specific diagnostic infrastructure and operational issues that must be confronted to achieve the technical and programmatic objectives of the ZR Project. In contrast to the activity of new diagnostic development to be supported by additional program funds, many of the diagnostic infrastructure issues identified here must be resolved within the budget and resources of the ZR Project.

IV.2. Redesign of the Diagnostic Platform Structure

As a result of the redesign of the water section pulse forming system (PFS) for ZR, the current collection of individual boats and platforms supporting the diagnostics for each LOS must be modified. The specific arrangement of diagnostic support platforms must be resolved as part of the ZR design process, but the general design goal should be for much more mechanically stable platforms with increased working space to facilitate rapid diagnostic setup and alignment. While the requirements for pulsed power maintenance access seem to rule out the use of a single mezzanine serving all radial lines-of-sight, it may be possible to provide platforms that serve all lines-of-sight within a 40° sector, with more space, improved access to the diagnostics, and common electrical (power, detector biasing, fast and slow triggering, remote operation and monitoring, high and low bandwidth recording, and common timing), vacuum, and LOS alignment utilities. This upgrade to the diagnostic platform structure will be accomplished within the ZR Project budget.

IV.3. Centralized Screen Boxes

A plan is being considered as part of the ZR Project to replace the multiple small screen boxes (Fig. 11) that provide local shielding for EMP sensitive diagnostic instrumentation on each LOS with three large centralized screen rooms providing the basic utilities and sufficient reserve utility capacity to support the diagnostics of several LOS sectors. The on-axis diagnostics package would also have to be supported within this framework. Centralized screen rooms with standardized utilities will require the

commitment of dedicated operations personnel to maintain and modify the common infrastructure. In addition, a plan should be considered for incorporating low EMP sensitivity diagnostic equipment such as fast valve controllers, MCP pulsers, Turbo pump controllers, vacuum gauges, and gatevalve controllers into separate screen or Hoffman boxes, to provide the necessary space and localization for the different LOS's.

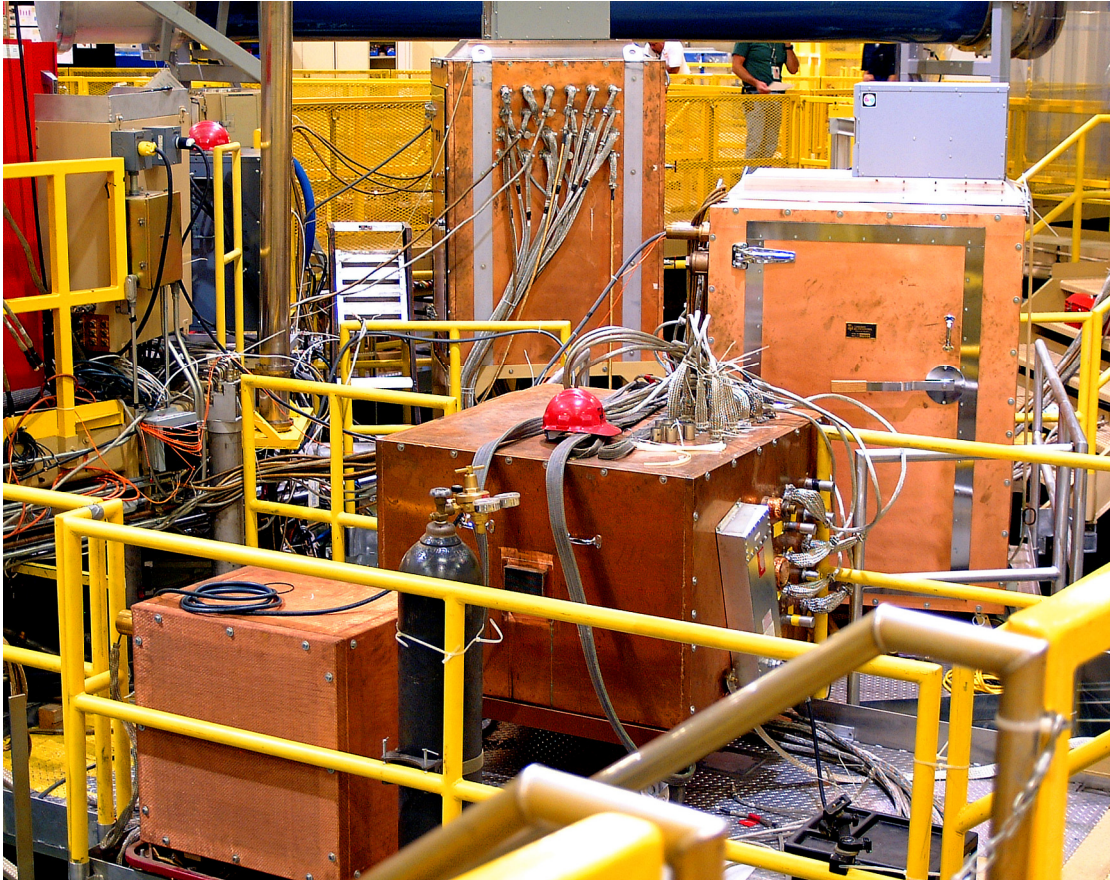


Fig. 11. View of small individual screen boxes supporting LOS 17/18 and LOS 21/22 diagnostic instruments.

The centralized screen rooms would have to be positioned above the diagnostic mounting platforms to maintain short signal cable runs and avoid bandwidth and ground loop problems. Extra care must be taken with cable management within a centralized screen room to avoid injecting noise into trigger signals. Part of each screen room would have to be partitioned off for streak cameras, which must be aligned in the dark. Adequate cooling would have to be provided for these large screen rooms. A chilled water system able to maintain the EMP integrity of the screen room would eliminate the dumping of hot air into the highbay. Such a chilled water system would require interlocks to shut down equipment in the event of a cooling system failure and some redundant backup capacity to prevent a failure of the common supply system from bringing down all screen rooms. All screen rooms should be shock mounted to decouple resident optical instruments from preshot vibration.

A medium-sized screen room already in place near the center section at LOS 9/10 (Fig. 12) is dedicated to the support of fiber-optic-coupled and open-beam-coupled optical diagnostics (single-point VISAR, line VISAR, active shock breakout, and laser interferometry) for shock physics and laser plasma probe measurements. Among the specialized utilities associated with this screen room is a 440-V 3-phase AC line to run the RF power supply for inductive preheating of samples for dynamic material properties studies. This screen room should be retained or enhanced for operation on ZR.

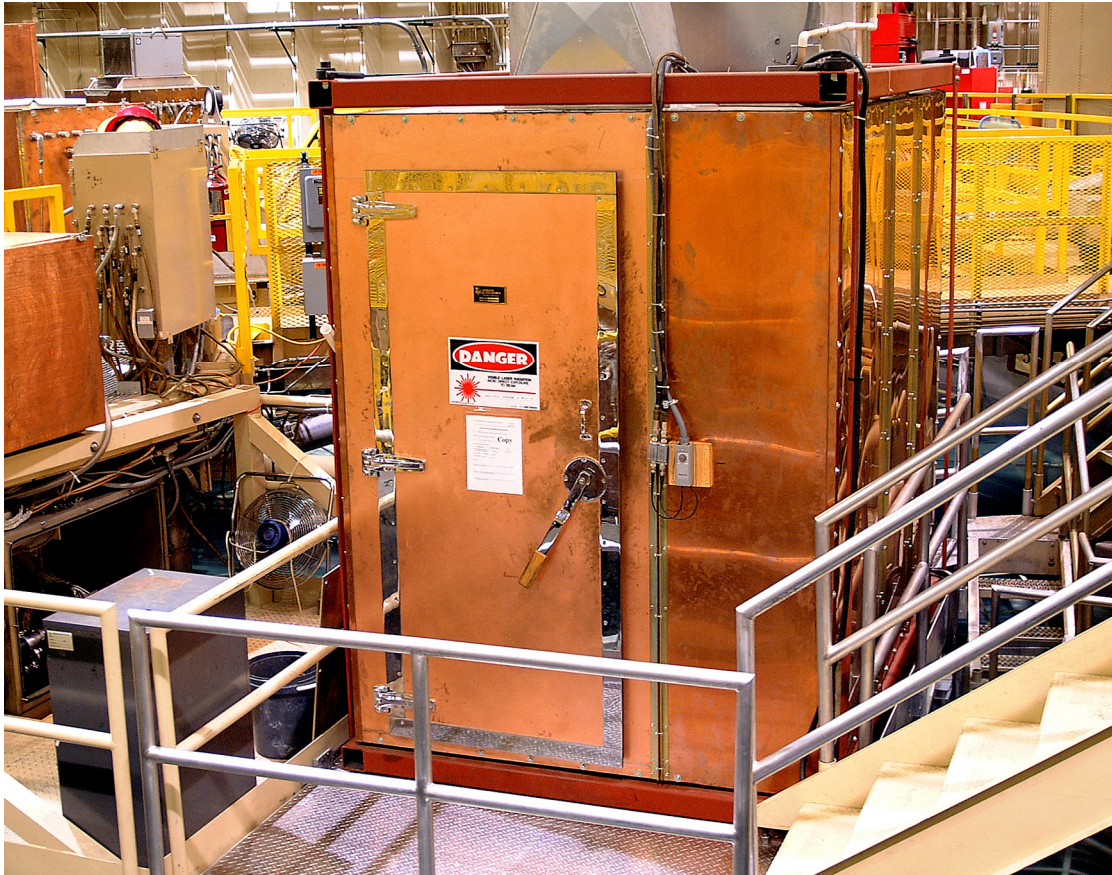


Fig. 12. Medium-sized walk-in screen room for shock physics and laser plasma probe instrumentation.

One alternative to three large screen rooms would be the grouping of some of the smaller existing screen boxes together into moderate size screen boxes or walk-in screen rooms serving all the diagnostic requirements of a single LOS sector. A second alternative would be a modified version of the existing system of multiple screen boxes for each LOS that improves upon the flexibility of the present arrangement. Instrumentation could be grouped according to function and housed in a mixture of: (1) fixed, walk-in screen rooms serving a particular local requirement for large instruments (streak cameras, spectrographs, VISARS, etc.); and (2) standardized small, modular, portable screen boxes for digitizers, delay generators, and power supplies that would allow for straightforward isolation from trigger noise and permit movement of electronics between LOS locations as diagnostic requirements change.

The process leading to a decision on the screen room architecture for ZR should be driven by requirements for pulsed power maintenance and diagnostic LOS access.

IV.4. Radial LOS Access

On Z, there are currently nine primary radial (side-on) LOS pipes at 40° intervals around the target chamber vacuum spool, each viewing the z-pinch load area at a polar angle of 12° above the horizontal plane to provide access to the diagnostics above the water level of the Z water section. Each LOS pipe is located in the center of an open sector between the nine hydraulic clamps securing the Z vacuum insulator stack. The primary LOS pipes generally branch into several smaller secondary pipes supporting individual diagnostic instruments (Figs. 13, 14). Each LOS is permanently assigned and adapted to the unique requirements of a particular diagnostic set and all available radial LOS pipes are currently occupied (see Appendix A1).

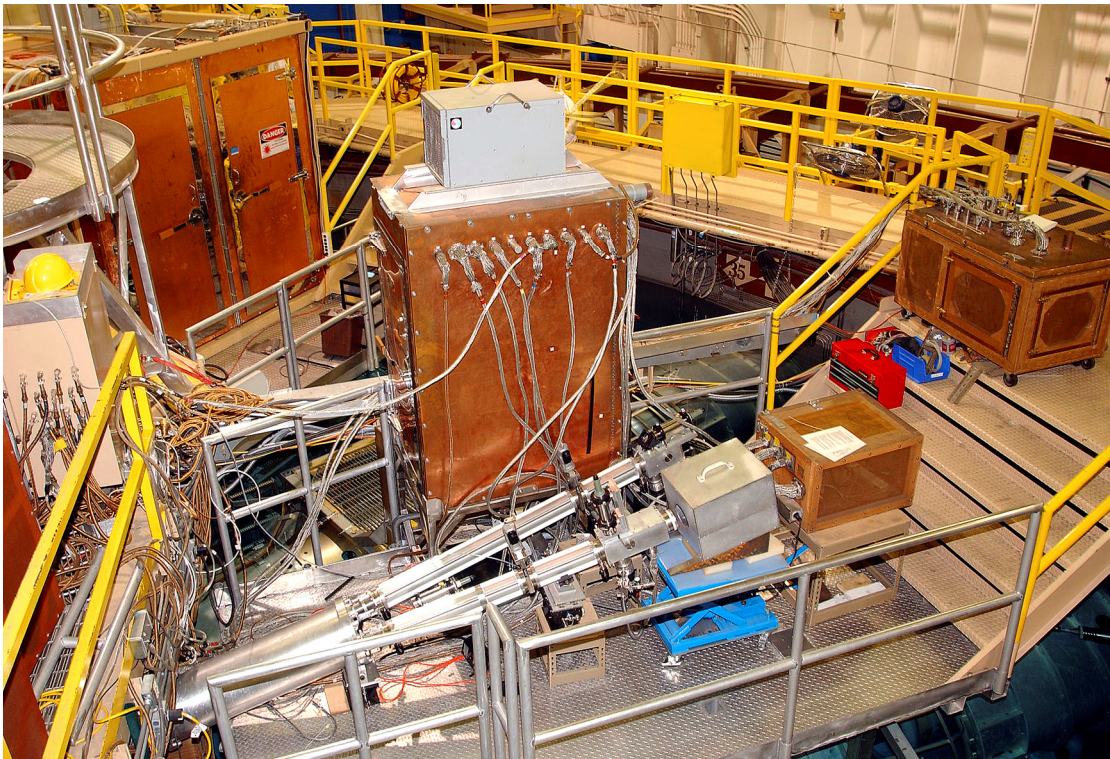


Fig. 13. Radial LOS pipes, instruments, and screen boxes for developmental LOS 1/2.

There is a critical need on ZR for more and flexible radial diagnostic access. Multiple keV diagnostic lines-of-sight are needed to fully characterize the z-pinch radiation distribution. There must also be flexibility in the location of diagnostics so that a full complement of pinch power and hohlraum temperature measurements can be performed on ZPDH double-ended hohlraum shots using the ZBL backlighter. These experiments will require 9–12 LOS diagnostic ports in addition to clear access to the ZBL entrance and exit ports for the x-ray conversion foil and the close-in (in-chamber) x-ray

imaging camera system. Similar requirements with different constraints would be imposed by the use of ZBL with monochromatic crystal imaging. The location of the diagnostic LOS ports would be driven by the ZBL aperture locations and by the need to maintain maximum azimuthal spacing between diagnostic apertures in the double-pinch load configuration to optimize power flow. In addition to multiple sets of existing core diagnostics, new diagnostics under development for ZR, as well as temporary, experiment-specific diagnostics, will require additional LOS access.

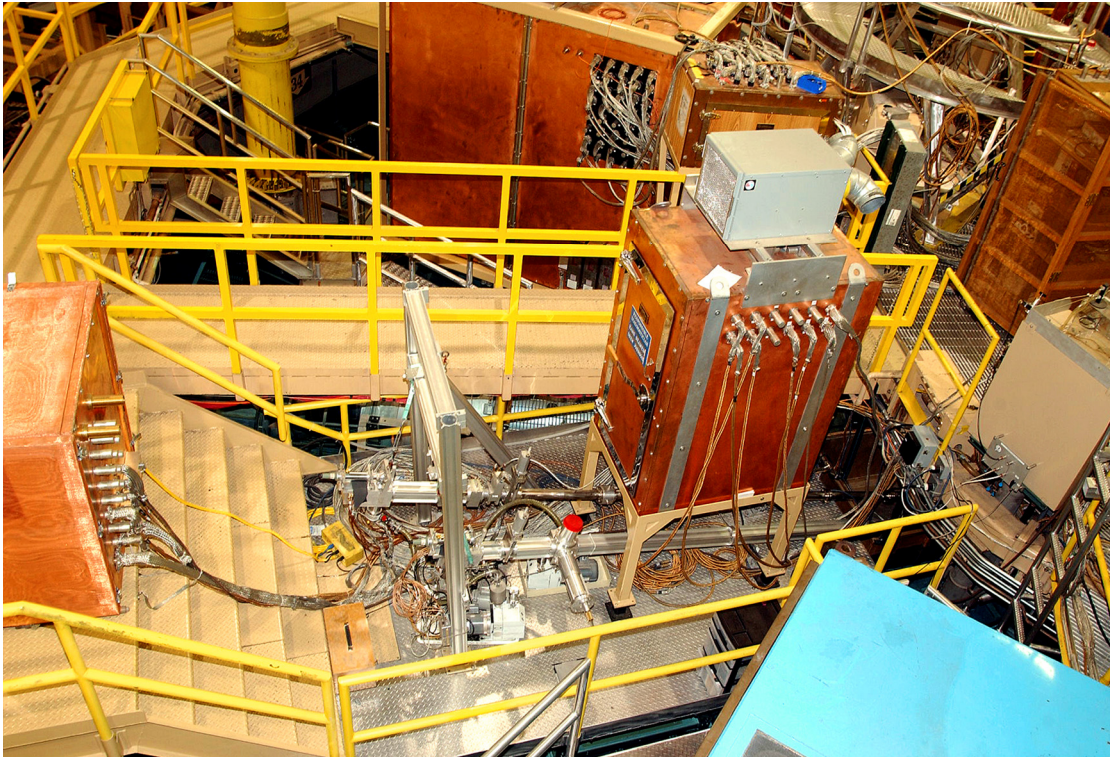


Fig. 14. LOS pipes, diagnostics, and supporting screen boxes on LOS 29/30.

Without a substantial mechanical redesign of the accelerator beyond the scope of the present ZR Project plan, primary LOS pipe access is limited by the location of the vacuum stack hydraulic clamps to the 9 open sectors at 40° intervals. While some core diagnostics packages with unique requirements will remain at a fixed position, there must be more primary LOS pipes at a larger range of azimuthal angles with common mounting fixtures and access to common electrical, vacuum, and signal conditioning utilities to support the flexible location of diagnostic instruments. Existing diagnostics packages will also require modification for compatibility with common diagnostic mounting fixtures. The most adaptable LOS arrangement would consist of large-area square mounting ports on the vacuum spool to which single or multiple large-area primary LOS pipes could be attached. An alternative would be to provide two large-area primary LOS mounting ports in each sector for a total of 18 primary LOS ports. The arrangement of LOS pipe access must be worked out as part of the ZR design process to support the matrix of anticipated requirements of the experimental groups using ZR.

IV.5. Diagnostic Insertion Manipulators (DIMs)

The Diagnostic Insertion Manipulator (DIM) is a device for inserting and accurately positioning diagnostic packages into large spherical laser target chambers that require retraction of the instruments for chamber interior cleaning and maintenance [87]. DIMs with common design and in several sizes have been developed for use on target chambers at the Nova, OMEGA, and NIF facilities (Fig. 15) to enable the exchange of manipulator diagnostics packages between the fusion laboratories (LLNL, LLE, LANL, SNL, CEA, AWE). The DIM consists of a vacuum housing, an extension tube which is inserted into the chamber, a diagnostic cart which can accommodate a wide variety of diagnostic packages, and an umbilical cable which carries all of the diagnostic utilities (high bandwidth coaxial cables, fiber optic cables, power and control cables, and liquid or gas cooling lines) and attaches to the diagnostic cart.

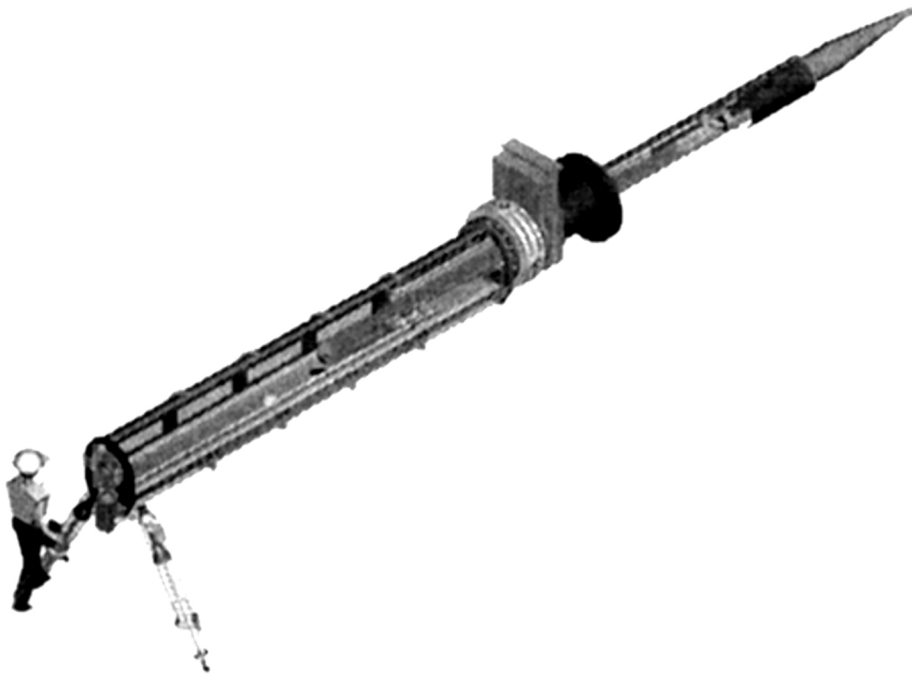


Fig. 15. NIF diagnostic instrument manipulator (DIM).

DIMs are not an absolute requirement for fielding diagnostics on ZR because of the relatively small diameter, open design of the cylindrical target chamber and the refurbishment procedure which requires the complete removal of all in-chamber and on-axis diagnostics, while providing for fixed installation of radial diagnostics at 5-30 m outside of the chamber. But DIMs are a very real requirement for active collaboration with the other fusion laboratories, permitting the efficient exchange of diagnostics for collaborative experiments and testing. It is a large advantage within the fusion

community to be able to develop diagnostics on one facility that can be used on another. For example, diagnostics packages could be brought to ZR for EMP and debris mitigation tests before use on NIF, and diagnostics developed for NIF could be used on experiments on ZR. There is also a need to position and accurately align SNL spectroscopy diagnostics below the water line, near the target chamber wall, with an insertion unit of some kind.

To provide a DIM capability on ZR, it is recommended that at least two radial 12° diagnostic ports should be included in the ZR LOS access design that are compatible with an appropriate, widely-used version of a DIM module, such as the TIM (ten-inch manipulator). Design and cost considerations should be investigated as part of ZR diagnostic development with the goal of providing two complete DIM modules with full optical communication and internal battery packs to allow the use of any ICF program diagnostic on ZR without modification by FY06. Shock isolation will be required since most ICF diagnostics packages will not have such shock mitigation built in. Survivability will be a critical issue for using existing ICF instruments without modification. This may preclude their use on ZR and should be examined. NIF instrument packages should already be designed for survivability in the ZR blast environment.

IV.6. Extension of Radial LOS Pipe Lengths

An increase in the peak pinch power for a standard wire array load from 230 TW on Z to 350 TW on ZR will require an increase in LOS pipe length for those radial diagnostics operating at or near their upper flux limits. LOS 5/6, the longest LOS pipe assembly housing z-pinch power diagnostics for maximum pinch power measurements, is most critically affected by this advance in ZR capability. TGS silicon photodiode signals, for example, are already too high on the most intense Z shots and the LOS extends close to the highbay wall, making a length extension from 26 m to 35 m impossible without penetrating the wall or rotating LOS 5/6 azimuthally toward the corner of the highbay. The bolometers and PCDs, presently at 19 m, should be moved back to about 26 m, a modification which can be easily accomplished with the new diagnostic support structure recently installed on LOS 5/6. The TEP (Total Energy and Power) diagnostic was designed with a flux limit of 350 TW and should not require an LOS extension.

Other z-pinch power diagnostics, such as those on LOS 17/18, LOS 21/22, and LOS 29/30 at ~ 10 m for measurements of double z-pinch x-ray production, hohlraum wall temperatures, and other applications involving less intense source configurations, may require LOS extensions to remain fully functional at increased flux levels on ZR. This should not be a fundamental problem. The length of LOS pipes for ZR must be determined as part of the LOS access design process. Diagnostic LOS length becomes an issue when locating large centralized screen rooms to minimize the length of signal cable runs.

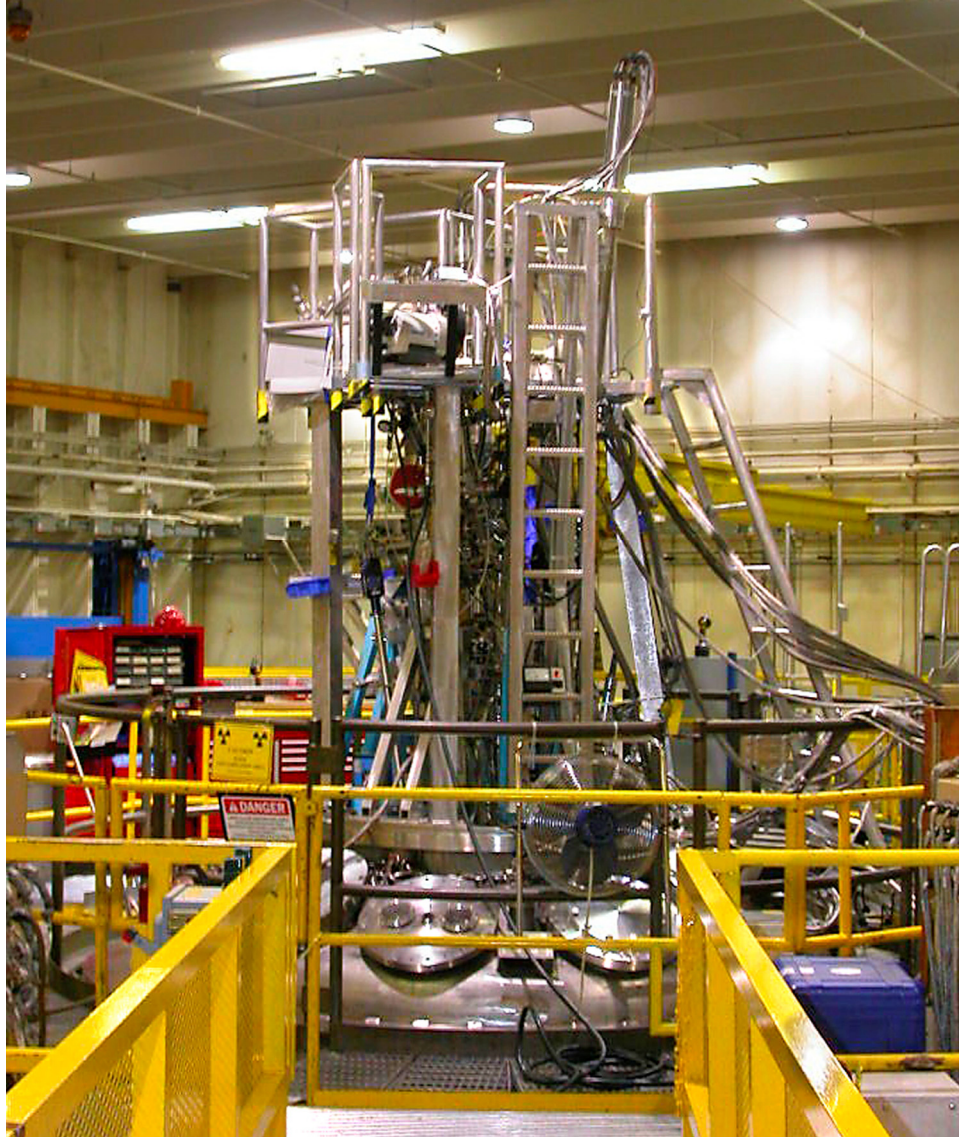


Fig. 16. Axial diagnostics package mounted on Z.

IV.7. Axial LOS Access

The present axial diagnostics package [40,88] consists of a close-packed array of LOS pipes, clustered around the z-pinch axis and terminating in diagnostic instrument heads just below the crane cross beam (Figs. 16, 17). Modifications to this configuration will be required for ZR. The LOS pipes for some power diagnostics will need to be extended beyond the height of the crane to avoid overdriving the diagnostics at the higher flux levels of ZR. Extension pipes with diagnostic heads will have to be mounted after the crane is removed. There is a need for a long on-axis (0°) neutron TOF LOS pipe that extends through the roof of the Building 983 highbay, imposing additional constraints on axial package assembly.

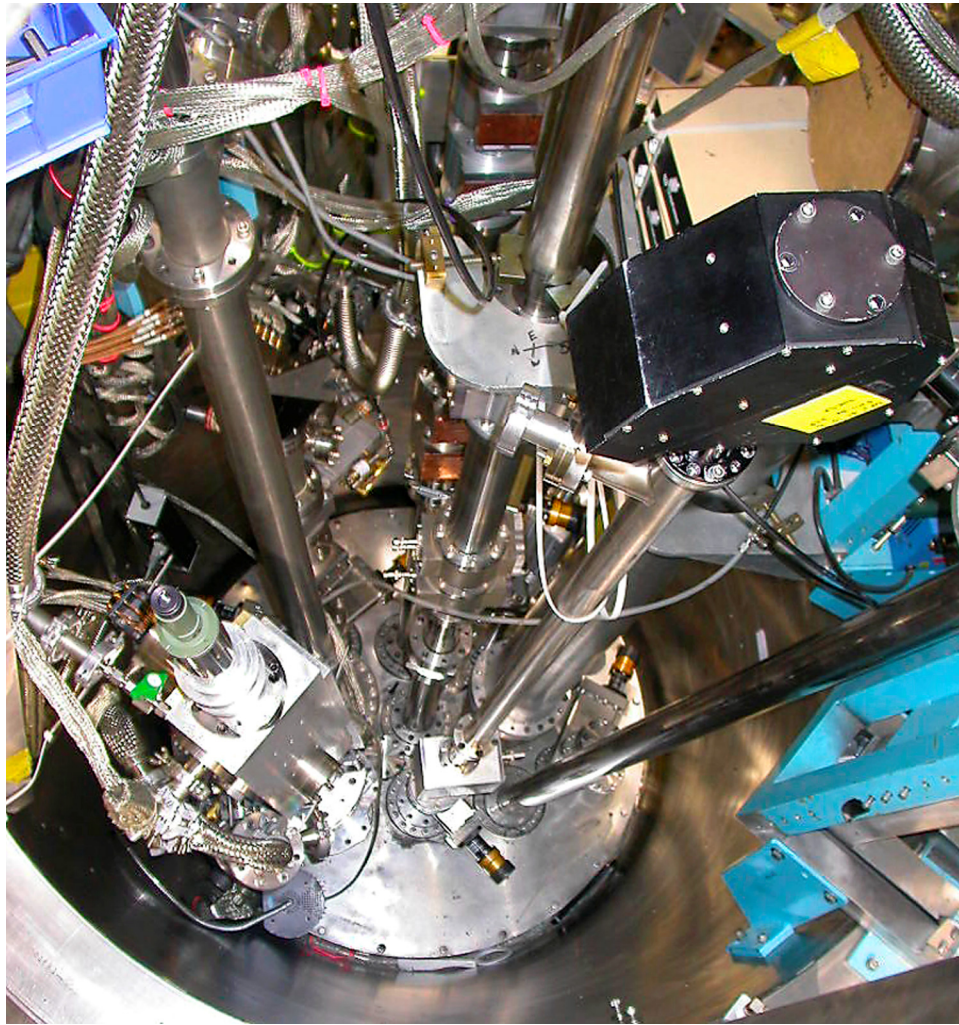


Fig. 17. Axial diagnostics and alignment hardware on LOS pipes.

Axial imaging and spectroscopy diagnostics with improved spatial and temporal resolution will have to be mounted closer to the z-pinch source, with LOS pipes extending into the target chamber, to achieve adequate photon flux at the detector plane. A reentrant array of diagnostic snouts converging on the load will introduce packing factor and survivability concerns. To the extent possible, compatibility should be maintained between the on-axis diagnostic package and the off-axis ZBL FOA.

There also exists a need to improve access for bottom-mounted diagnostics (Figs. 18, 19) so that a more complete package of core diagnostics can be fielded on the bottom side of ZR.

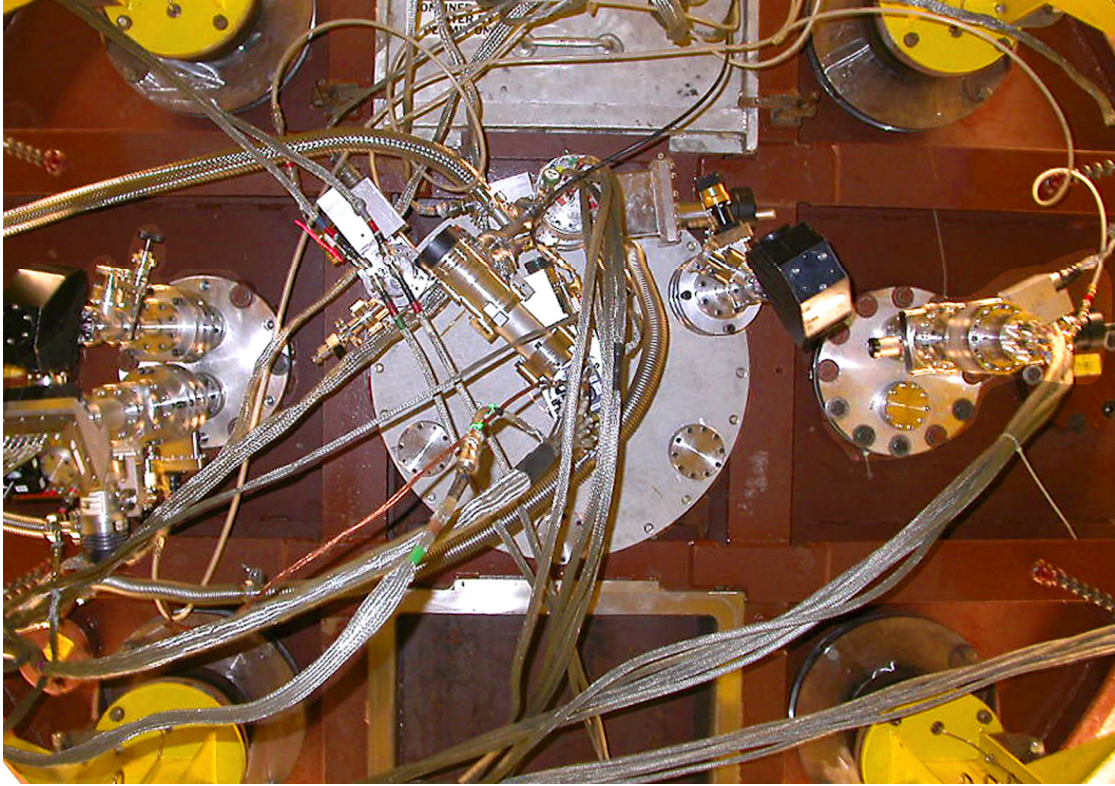


Fig. 18. Axial diagnostics package on bottom of Z.

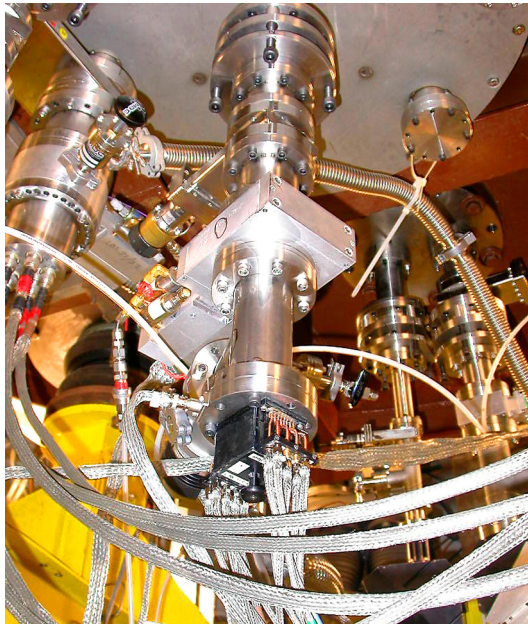


Fig. 19. Axial x-ray pinhole camera at 0° on the bottom of Z.

IV.8. On-Axis Debris Mitigation

On ZR, the total radiated x-ray energy from the standard wire array load will increase from 1.6 MJ to 2.7 MJ. This energy is ultimately dissipated in the form of radiation, hot vapor, molten metal, and solid shrapnel expanding out of the load region. An exclusion zone exists in which most load and diagnostic components will be vaporized by the x-ray flux. Survivability of diagnostics outside of this exclusion zone is a critical issue for ZR. Debris mitigation is typically accomplished using a combination of blast shields, baffles, and fast closing valves, and is a particular problem for on-axis diagnostics because of the selective jetting of hot material along the z-pinch axis in response to megagauss radial magnetic field pressures generated in the pinch. Debris mitigation for axial diagnostics will require specific attention, careful design, and testing. The combination of a more energetic load accelerating more debris mass to higher velocities and the location of imaging and spectroscopy diagnostics closer to the source in a reentrant geometry to meet the need for higher spatial and temporal resolution creates the potential for increased damage to apertures, fast shutters, and the diagnostic itself in the event of a fast valve timing failure. Inspection and replacement of shield components will affect diagnostic turn-around time. Reliable fast-valve operation, the utilization of electromagnetic shutters, innovative baffle design, and the use of gas curtain and multiple filter techniques will become essential for on-axis diagnostic survival.

IV.9. Target Chamber Vacuum Feedthrough Ports

At present, there are several ports in the upper and lower wall of the cylindrical target chamber that provide vacuum feedthrough access for fiber optics, high bandwidth electrical signal cables, power cables for vacuum lights, open-beam optical lines-of-sight, and cryogenic system transfer lines and control cables. Shock physics experiments, which use high magnetic pressures generated in short circuit loads for the study of dynamic material properties, have their own unique set of fiber-optic-coupled and open-beam optical diagnostics that rely heavily on vacuum feedthrough port access while making no use whatsoever of the 12° radial LOS diagnostic ports used in wire array load experiments. On Z, two ports are completely occupied with fiber optic vacuum feedthroughs for multiple VISAR, active shock breakout, and visible light spectroscopy, and a third port provides open beam optical access to the large LOS 9/10 screenroom for a line VISAR diagnostic and laser plasma probe optics.

On ZR, it is recommended that vacuum feedthrough access to the target chamber be increased to include two optical open-beam LOS ports designed to accept periscope mirror turning boxes and located in line with the dedicated LOS 9/10 screen room. Fiber optic feedthroughs will be required for approximately twice as many fibers as presently in use. Some of the new feedthroughs will be used to support additional single-point VISAR channels or for new fiber-coupled diagnostics such as optical pyrometers for temperature measurements in sample preheat experiments. The present cryogenics port for cryogenic transfer and gas lines, required to condense liquified gas samples for EOS measurements, should be retained at its present position if possible.

Additional vacuum feedthrough access should be provided by enlarging existing ports or adding new ports above the water level. However, there is limited space to add

new ports with external working access that does not interfere with the target chamber cryopumps.

IV.10. Diagnostic Timing

One of the most critical requirements for ZR diagnostics, along with improved spatial resolution, is better timing synchronization between command fire and pinch stagnation, resulting in a reduction in diagnostic trigger signal jitter to the ± 1 ns level with respect to peak radiation power. The dominant source of timing jitter on Z is the statistical nature of the firing of the 36 output gas switches in the final stage of pulse compression that affects the current waveform and time of peak pinch power for a wire array implosion. For most diagnostics, fast trigger signals are generated from an average of four self-break water switch voltage signals captured downstream of the gas switches well before pinch stagnation. When the ZBL laser is used as a backlighting diagnostic, the Z machine command fire and gas switch laser trigger signals are derived from the earlier ZBL laser command fire to control the synchronization between pinch stagnation and the ZBL laser pulses. Up to the end of 2002, the gas switches were triggered with a common laser. At that time, the 1σ shot-to-shot variation in timing between the diagnostic trigger (from either trigger source) and peak pinch power for “identical” wire array implosions was about ± 3.9 ns, resulting from a combination of gas switch laser trigger jitter of 3 ns and the power flow jitter of an array of identically triggered switches of 1.5 ns.

A diagnostic trigger jitter on Z of > 3 ns poses a significant problem for a large class of experiments involving transient phenomena that occur in a few ns time window or that impose stringent requirements on diagnostic synchronization with the pinch implosion. Good examples are: (1) fast ignitor experiments [81], where the maximum density of the compressed fuel occurs within a window of < 2 ns and a precisely-timed petawatt laser pulse must be applied within that window for fuel ignition; (2) x-ray photoionization experiments with thin foils [79], where the desired photoionized plasma equilibrium is achieved only transiently in a 2 ns window; and (3) imploded core x-ray imaging or spectroscopy using a high time resolution gated framing camera or streak camera with an active window of 2 – 4 ns. Ideally, timing jitter of 200 ps would be desirable for synchronization of ZR with a petawatt laser and a diagnostic jitter less than 500 ps would be useful for capsule implosion experiments. However, there is sufficient variation in the z-pinch implosion itself, resulting from variations in mechanical assembly and power coupling to nominally identical wire arrays, to make control of pinch power timing with this precision unrealistic. A more realistic goal is to develop a laser trigger system and laser-triggered output switches capable of sub-nanosecond timing jitter, resulting in a current waveform that is sufficiently reproducible to yield a command fire to pinch stagnation jitter of ± 1 ns.

Diagnostic timing jitter can be reduced by improving (1) gas switch laser trigger jitter and (2) gas switch trigger spread. The first step toward reduced diagnostic timing jitter has already been accomplished through a program for individual laser switch triggering, implemented before ZR construction with the purchase of lasers in FY02 and installation in FY03. By triggering each output switch individually with its own laser, systematic variations in individual switch performance can be tuned out efficiently through adjustments in laser timing and intensity, and the laser trigger contribution to

output switch jitter reduced to the level of ± 500 ps or less. Individual laser switch triggers also provide a precision current pulse shaping capability for isentropic compression experiments. A second step toward reduced diagnostic timing jitter would be reduction of the power flow jitter by improved ZR output switch design to reduce switch spread and by improved reproducibility of waveforms applied to the output switches through control of PFS MITL mechanical tolerances. The power flow jitter for an identically triggered array of output switches would have to be reduced to the level of 1 ns or less, a formidable requirement.

If output switch jitter can be significantly reduced, the quality and jitter of the water switch signals used to generate the diagnostic trigger should improve. A better approach at this point might be to derive the diagnostic trigger directly from the command fire signal with 200 ps accuracy, capturing the reduction of jitter between command fire and pinch stagnation without dependence on water switch waveform averages. In addition to providing improved diagnostic trigger timing with adequate trigger lead time to support any function, this approach would provide a dry-run trigger system for diagnostic testing during preshot preparation and maintenance, independent of accelerator and laser trigger systems, with synchronization of all systems to within ± 1 ns for the shot. A reduction in diagnostic timing jitter should improve the quality of data from all gated x-ray detectors and allow improved time resolution for streak camera records of transient events. Further improvement in data can be achieved by expanding the use of multiple-gated diagnostics, covering the event window with several frames, or in the case of ZBL backlighting, by using multiple laser pulses.

It may also be possible to obtain a diagnostic timing signal with jitter with respect to pinch stagnation of less than ± 1 ns from a highly reproducible load B-dot signal measured close to the imploding wire array. Because of the short lead time available from such a trigger source, this trigger would be most useful for close-in diagnostics and/or relatively late events associated with pinch stagnation or peak pressure generation.

Pre-triggers resulting in loss of data can be eliminated by remote reset and arming capabilities to be implemented in the ZR Project (see Sec. IV.13) and by use of trigger veto modules to reject false noise triggers that fall outside a preset event window with respect to command fire.

IV.11. Vacuum System Issues

To eliminate the need for an individual roughing pump for each diagnostic, with all of the associated space, vibration, and maintenance issues, it is recommended that a common roughing system, consisting of a 10 mTorr vacuum manifold accessible from the diagnostics platforms, should be implemented on ZR. However, the decision to use a common roughing system, rather than individual roughing pumps, has certain drawbacks and is still being debated. For a common roughing system to work, each diagnostic must have a manual gate valve at the point of connection to the target chamber and must be leak tested prior to opening to the target chamber, preferably in the diagnostics lab prior to mounting. Helium gas ports should be provided at each diagnostic station for leak checking. Nitrogen gas ports should also be provided for fast valve operation. Oil-sealed roughing pumps are a concern for contamination of diagnostics and power flow electrode surfaces. Wherever possible, dry-seal roughing pumps should be used.

The existing array of cryopumps on the target chamber, supported by cryopumps on the longer LOS pipes and turbopumps on the individual diagnostics, will provide high vacuum on ZR. There is no room for more or larger cryopumps on the present target chamber, which will be retained and modified for use on ZR. With the present system, vacuums in the range of 2.5×10^{-5} Torr for standard shots can be reached in 90 minutes and vacuums of about 8×10^{-6} Torr required for cryogenic experiments can be achieved in 180 minutes. By precooling of the helium delivered to the cryopump cold head, the hivac pumpdown time can be reduced by 40 minutes.

IV.12. Diagnostic Operational Issues

Of equal importance to developing new diagnostics for ZR is achieving reliable operation of the existing core diagnostics. A reliable set of instruments with a high data yield is required to avoid critical gaps in experimental data. This will be accomplished only by well-defined ownership of diagnostics by technicians with adequate backup of key personnel, involvement of physicists in diagnostic setup and data quality control, well-defined operating procedures, and adequate calibration, maintenance, and documentation of each diagnostic. Problems in the past have resulted from the lack of adequate change control, the tracking through documentation and communication of small changes in diagnostic setup and timing. Nor has the quality of information produced by the diagnostics been monitored in any systematic way. The measurement of data quality through periodic data reviews will result in continuous improvement of diagnostic performance.

IV.13. Remote Control of Diagnostics

The capability for full remote control and monitoring of all diagnostics should be implemented as part of the ZR Project. Fast valves, gate valves, high voltage biasing, film advance, arming and reset, vacuum monitoring, and other diagnostic control functions can all be remotely operated and monitored to eliminate the need for diagnosticians to reenter the highbay following trigger checks. Precision alignment of diagnostics such as silicon diode and XRD arrays with apertures and baffles should also be performed remotely wherever possible using video monitors with computer control of LOS and baffle translation stages. Arming and shutter opening should be performed remotely to avoid the situation where manually controlled diagnostics must sit armed for long periods before a shot. Full remote control of all diagnostics would significantly speed up the shot sequence and improve the reliability of diagnostic operation. Additional space in the data acquisition screen room area or diagnostics preparation lab will have to be allocated for diagnostic remote control and monitoring.

IV.14. Fiber-coupled Vacuum Illumination Systems

The present vacuum lights, used inside the Z target chamber for final diagnostic alignment under vacuum, burn out easily, typically after pumpdown, and require venting for bulb replacement. On ZR, a fiber-coupled vacuum illumination system should be used to improve reliability and turn-around time. Such a system would consist of a large

fiber bundle bringing light from an external source through a vacuum feedthrough into the target chamber where the fiber bundle would branch into separate sources for the individual LOS apertures.

IV.15. Improved Diagnostic Turn-around Time

One goal of the ZR Project is to provide infrastructure with the capability to support 400 shots per year. There is a need to identify methods to increase the efficiency of diagnostic operations and to reduce diagnostic turn-around time to accommodate this increased shot rate. One step in this direction would be to build the capability into each diagnostic (XRDs, PCDs, bolometers, etc.) wherever possible to inspect filters and pinholes and to perform alignments without breaking vacuum. In addition, diagnostic designs should be implemented wherever possible to minimize component damage from debris.

IV.16. Center Section Mock-up

There exists a need for a complete mockup of the center section upper and lower MITLs to which load hardware can be added to check the setup of optical and other close-in diagnostics prior to installation on ZR. Such an assembly in the highbay or other suitable location would greatly improve the turn-around time for initial installation of complex optical imaging and other in-chamber diagnostics systems. There is also the need for a generic set of threaded mounting holes at large radius on the upper anode plate in the target chamber to facilitate the mounting of close-in diagnostics without the need for custom modifications to the anode during shot setup.

IV.17. Tritium Use on ZR

Higher thermonuclear neutron yields should result from DT capsule implosions compared to DD reactions, permitting the use of a wider range of neutron diagnostics. Procedures should be developed for rapid and appropriate tritium handling and decontamination for ICF capsule implosion experiments on ZR. Initial steps have been taken to identify and meet the requirements for tritium handling on Z and ZR, but the first experiments to gain experience with gas-filled capsule implosions will be performed using pure deuterium gas and low detection threshold total yield and TOF diagnostics.

IV.18. DAS Screenroom Space Utilization

There is a general requirement for more space in the DAS screenroom area to accommodate additional VISARs, lasers, and a cryogenics control system.

IV.19. Conceptual Design Study for ZR Double-Sided-Drive Configuration

A conceptual design study should be carried out to evaluate the feasibility of a double-sided power feed configuration for ZPDH fuel capsule implosion experiments on ZR. The requirement for a double-sided drive would be triggered at some future point by the inability to achieve acceptable power balance and timing, diagnostic access, or cryogenic target access with the single-sided-feed configuration for ICF double-ended hohlraum capsule experiments requiring highly reproducible top-bottom drive symmetry. A full design study is beyond the scope of the ZR Project and would need to be funded as part of the ICF Program.

A double-sided feed, if required, must be compatible with the single-sided feed components, enabling cost-effective conversion of the ZR PFS and insulator stack from the single-sided feed. A two-side current feed would be required, delivering at least 14 MA per side to allow an 80-eV secondary drive temperature, with some method of current smoothing between the two transmission line feeds over all 36 water lines so that the current pulses are identical within $\pm 1\%$ on each side. Current smoothing between the two transmission line feeds would ensure good radiation symmetry by providing power and timing balance between the upper and lower primary hohlraum sources driving the central secondary hohlraum containing the implosion capsule. Hardware should be designed allowing efficient changeover between single- and double-sided drive with no longer than 3 weeks in either direction. Many experiments on ZR will still require the single-sided feed configuration, but it is anticipated that two-sided power feed ICF experiments, if necessary, would be initiated in the 2008-2009 period for 4 – 6 months per year.

Radial diagnostic access for a double-sided-feed ZPDH will be limited to a 12-inch-high space at the midplane between transmission lines to avoid an unacceptable penalty in inductance. This space would accommodate diagnostic access by a limited number of 10-inch-diameter LOS pipes at 0° penetrating the water and Marx generator sections to the tank exterior. 0° radial access would also be desirable for neutron diagnostics. A retractable diagnostic insertion manipulator (DIM) [87] of some type would be required for radial diagnostic operation in this arrangement. There is also a radial access requirement for a cryogenic system to insert frozen DT fuel capsules into the secondary hohlraum. Core radial diagnostics required for high convergence DT capsule implosions must be identified as part of the process to define diagnostic access requirements for the double-sided feed configuration. Insulator stack, transmission line, water line, and diagnostic LOS retrofit hardware will not be procured as part of the ZR Project, but will require a separate funding request.

IV. 20. Conceptual Design Study for Petawatt Laser Compatibility

A conceptual design study should also be carried out to define future modifications of ZR required to incorporate petawatt laser infrastructure and trigger timing accuracy into ZR for a Fast Ignitor program. Fast ignitor [89-96] capsule implosion symmetry experiments [97] and efforts to develop a short pulse petawatt laser capability around ZBL laser facility components are already underway. This design study would enable the cost-effective adaptation of ZR to a significant future opportunity for fast ignition research with z-pinch drivers. Such a design study is beyond the present scope of the ZR Project and would need to be funded as part of a petawatt laser development program.

A single-sided-drive configuration is presently being explored to achieve the necessary drive symmetry for fast ignition with a z pinch, so a fast ignitor program on ZR may not necessarily be tied to the implementation of a double-sided-drive load configuration. Whether fast ignitor experiments are performed in single- or double-sided drive, the infrastructure should be provided for radial diagnostic access and for cryogenic fuel capsule handling, with remote access through one LOS. Cryogenic targets are important because of the possibility of compression to higher density for a given laser energy. Another primary requirement for future fast ignition work is the ability to synchronize the laser command fire trigger and the ZR z-pinch peak radiation power to within ± 1 ns or less.

V. Diagnostics Calibration and Data Analysis Issues for ZR

V.1. Introduction

Accurate, reliable, traceable calibrations of x-ray and other diagnostics will contribute much to the quality of data and to the benchmarking of model simulations with experimental results obtained on ZR. Adequate calibration of the wide range of diagnostic instruments that will be fielded on ZR is a time-consuming, resource-intensive task and will require the dedicated allocation of resources beyond the level of effort on Z. With an increased shot rate and a greater quantity of diagnostic data generated on each shot, the organization and analysis of data from ZR experiments will also require increased attention.

This section contains a brief discussion of a number of specific diagnostic calibration and data analysis issues facing ZR.

V.2. Calibration of Z-pinch X-ray Energy and Power Diagnostics

Progress needs to be made in the characterization and absolute calibration of those core diagnostics used for measurement of the z-pinch x-ray energy and power, which include bolometers, calorimeters, XRDs, PCDs, TGSs, and the TEP diagnostic. The accuracy of these instruments is critical because their measurements provide the primary input for simulations of power flow, hohlraum performance, and other essential features of z-pinch experiments.

The accuracy of resistive bolometer measurements [67] is particularly important, because pinch power waveforms are obtained at present by normalizing XRD waveforms (and, in the future, TEP waveforms) to absolute bolometer energy measurements. Bolometers are high fluence, time-resolved fast-pulse x-ray diagnostics with flat spectral response whose calibration is derived from the intrinsic material properties and geometry of the resistance elements. Bolometers have a relatively simple and stable response compared to some other diagnostics and probably have the best potential among the core x-ray flux diagnostics for accurate absolute calibration. The ability to fabricate thin-film nickel bolometer elements with resistivity equal to that of bulk nickel has been demonstrated, as has the ability to control film deposition uniformity, masking, and aperture geometry to allow accurate and consistent measurement of the geometrical film parameters of thickness, width, and active length. Error bars on the geometric film parameters, resistivity, and specific heat, and on measurements of the bias current and resistive voltage change result in accuracy of about $\pm 10\%$ on absolute bolometer energy measurements at present. Efforts should continue to reduce the error bars on bolometer measurements to the $\pm 5\%$ level.

XRDs are large-area, fast-response soft x-ray flux diagnostics [68] whose sensitivities are appropriate for x-ray power measurements on Z and ZR without pinhole imaging. The vitreous carbon photocathodes and x-ray filters used in XRD arrays on Z

are calibrated between 150 and 5700 eV at the National Synchrotron Light Source (NSLS) facility at Brookhaven National Laboratory by Bechtel-Nevada (BN) personnel on a six-month basis. Some filters are characterized for thickness by α -spectroscopy energy loss measurements and then cross-calibrated with the NSLS-characterized filters. The $1\text{-}\sigma$ error bars are $\pm 10\text{-}15\%$ on photocathode sensitivity and $\pm 5\%$ on filter transmission, resulting in an overall error on channel response of $\pm 20\%$ that dominates the error in XRD measurements of peak pinch power. Stability of the detector response is an issue because of surface film formation and surface etching of the photocathodes in the Z shot environment. This is controlled by maintaining a clean preshot vacuum isolated from the main accelerator vacuum and by changing photocathodes every 20 shots. It is unlikely that the accuracy or stability of XRD detector response can be substantially improved in the high-shot-rate ZR environment. It is recommended that the present XRD calibration procedures be maintained and monitored to ensure at least the present level of XRD calibration accuracy.

Diamond photoconducting detectors (PCDs) [69-71] are primary x-ray flux diagnostics on Z that feature fast, stable, flat response out to about 6 keV with a rugged, readily cleanable surface and very limited sensitivity to bremsstrahlung radiation. Initial attempts to calibrate the PCDs with NSLS and dc Henke x-ray sources resulted in unacceptably large error bars because of the variation of detector response across the surface and the spatial nonuniformity of the calibration sources. Calibrations with a pulsed laser x-ray source at Sandia for a limited number of spectral points from 163 eV to 2 keV produced more satisfactory results, with $1\text{-}\sigma$ error bars on the response of the individual PCD elements of $\pm 15\%$ and an overall filtered channel response of about $\pm 20\%$. It is recommended that detector calibration work with the laser x-ray source be supported to provide absolute calibration of PCDs and that PCD array response be extended to 10 keV.

The TEP diagnostic is presently under development [72]. The calibration of this instrument will be based on the intrinsic response of the silicon p-i-n diodes, on an absolute calibration of the silicon diodes to address potential oxide thickness issues, and on cross calibration with the resistive bolometer array.

Calibration of the transmission grating spectrometer (TGS) depends on a calibration of the grating response as a function of the x-ray energy and on the intrinsic response of the silicon p-i-n diode detectors. The $1\text{-}\sigma$ error bars on the TGS channel response is about $\pm 20\%$. It is recommended that calibrations for TGS instruments be supported and improved, and that improvements in grating fabrication be implemented.

V.3. X-ray Crystal Calibration and Characterization

Except for the new spectrometer being developed by Bechtel-Nevada (Sec. III.6), crystal spectrometers are not calibrated for use on Z. It is recommended that additional support be provided for BN to absolutely calibrate the response of crystal spectrometers and to characterize crystal artifacts and distortions resulting in nonlinear dispersion.

V.4. Pulsed Laser X-ray Calibration Source

A pulsed laser x-ray calibration facility has been developed at Sandia [70] to provide a spatially uniform, monochromatic x-ray flux for calibration of PCDs and other diagnostics with adequate sensitivity to low intensity x-ray sources. A 1 ns FWHM pulse from a 1.5 J laser at 0.5 μm is used to vaporize and ionize an x-ray target, producing x-rays at a limited number of spectral points from 163 eV to 2 keV. The incident x-ray flux at the detector is measured with silicon p-i-n diode CCDs cross calibrated against flow proportional counters as an absolute standard to provide an absolute x-ray calibration capability. It is recommended that the pulsed laser facility receive continued support for calibrations requiring low intensity pulsed x rays with a spatially uniform x-ray flux. The potential also exists to use the ZBL as a pulsed laser x-ray calibrated source for diagnostics requiring higher intensity x rays.

V.5. MCP Characterization

The methodology has been developed for characterizing the response of MCPs including flat fielding, linearity, and spatial resolution of MCP-based x-ray detection systems used for x-ray pinhole imaging and other applications. Because of a lack of resources, these procedures are not being routinely applied and most MCP systems in use on Z have not been characterized. It is recommended that more resources be applied to the characterization of MCP-based detector systems to improve the accuracy of quantitative x-ray imaging data.

V.6. X-ray Film Calibration

There should be a general movement away from film toward high quality CCD cameras for recording x-ray images to facilitate remote control and rapid data recovery. However, there will still be applications of close-in x-ray imaging systems where the EMP and bremsstrahlung noise environment of ZR will make operation of CCD cameras highly problematic, or applications where very high spatial resolution is required. In these cases, film will remain the best choice as a recording medium. The only available absolute film calibrations are those from Henke [98] for a limited set of x-ray films available 20 years ago that are or may soon go out of production. It is recommended that additional support be provided, as required, for absolute calibration of local spectral response of x-ray films, possibly by BN using the NSLS facility at Brookhaven National Laboratory.

V.7. Searchable Data Base for ZR Shots

A searchable data base is required for ZR shots, containing basic load and experiment parameters, shot objective and category keywords, and links to the diagnostic setup database. This will allow efficient sorting of shots by category for rapid information retrieval and identification of trends. Responsibility for data entry can be

delegated to dedicated support staff who will collect the essential information for each shot from the principal investigator and other sources.

V.8. Data Analysis Procedures

An integrated set of data analysis procedures for the basic ZR diagnostics should be developed with staff member oversight. Data analysis could then be performed in a consistent manner immediately after each shot by personnel below the staff member level and made available for use by the experimenters. Individuals responsible for data analysis would also be responsible for tracking and documenting diagnostics changes and problems and for making minor modifications in data analysis procedures to accommodate new conditions and requirements. Diagnostic experts at the staff member level would be responsible for generating new data analysis procedures and for maintaining data analysis quality control through informal and formal data reviews. The well-documented set of basic data analysis procedures would be available to experimenters for independent verification and interactive extension of the data analysis if desired. This new process would provide continuity, consistency, and efficiency that is currently lacking in a process that is fragmented among multiple staff and technicians and not consistently documented.

It would also be desirable to have a well-defined process in place to unfold the more advanced diagnostics that are in general use. This would involve either consistent, definitive data analysis by a designated diagnostics expert for each instrument, or a well-documented support system (reference material, test cases, expert advice) for a set of data analysis procedures that an experimenter could master and use with confidence.

VI. Priorities and Budget

VI.1. Prioritized List of Recommendations

This section contains a prioritized list of recommendations for new ZR diagnostic development covering the first few years of ZR operation. A more extended discussion of these diagnostic requirements and related issues can be found in Section II. Improvements to existing core diagnostics described in Section III are part of an ongoing process that should be well advanced by the time ZR becomes operational and will not be considered here. The diagnostic infrastructure requirements discussed in Section IV are generally essential for the program and will not be further prioritized here, although the feasibility and ownership of certain infrastructure options are currently under debate.

Priority 1 Diagnostic Development

These are new diagnostics required in the near term after ZR becomes operational to characterize and utilize the increased shot capabilities for x-ray production and magnetic pressure generation, enhanced precision, and pulse shaping variability of the upgraded accelerator. These diagnostic capabilities can, in general, be developed prior to the construction phase of ZR and tested within the existing Z diagnostic infrastructure.

- Develop ZBL for operation at full design capabilities as a point projection backlighter, with 2 pulses of 500 J of less than 2 ns total duration, 25-35 μm laser spot size with adaptive optics, and up to 9-keV probe x rays.
- Develop a bent crystal monochromatic x-ray imaging system with spatial resolution of less than 10 μm , a 3-mm-diameter field of view, and x-ray probe energy to 6.18 keV.
- Develop high spatial resolution (20- μm) gated x-ray pinhole cameras with 80 ps time resolution for on-axis and side-on backlit imaging of dynamic hohlraum pellet implosions.
- Develop a bent crystal monochromatic x-ray imaging system with a large field of view for high spatial resolution x-ray imaging of z-pinch stagnation.
- Develop x-ray spectrometers with improved spatial resolution and 100 ps time resolution capable of operating close to the load.
- Develop fiber-optic-coupled UV spectrometers for dynamic materials properties studies.
- Develop the capability for fielding cross-calibrated, time-resolved x-ray spectrometers on two different lines-of-sight for opacity measurements.

- Develop a soft x-ray spectrometer with extended range to cover brightness temperature from 50 to 300 eV to study time-resolved spectral evolution of a x-ray emission area during both the z-pinch implosion and stagnation phases.
- Develop a hard x-ray spectrometer with a range of 10-100 keV to assess the hard x-ray background from z-pinch stagnation.
- Develop a high-sensitivity total neutron yield detector with a 5×10^6 neutron detection threshold.
- Develop a highly-collimated neutron TOF detector system with one on-axis and one side-on (12°) LOS.
- Improve time resolution of single-point VISARs from 1 ns to 100 ps and of line-imaging VISAR from 50 ps to 1 ps.
- Develop a full-field, gated multiframe VISAR for time-resolved 2-D measurements of particle velocity and shock breakout.
- Develop streaked imaging shock breakout diagnostic based on line-VISAR or direct optical imaging of a 1-D region with open-beam coupling.
- Develop laser probe diagnostics using refraction, reflection, absorption, and inverse Bremsstrahlung absorption of laser probe beams to characterize low density plasmas associated with z-pinch implosions, hohlraums, and complex hydrodynamics experiments.

Priority 2 Diagnostic Development

These are new diagnostics that will greatly enhance the quality of experiments on ZR, but which will require a more extended development period or the availability of the increased shot capabilities and diagnostic infrastructure of ZR for development and testing.

- Develop Kirkpatrick-Baez grazing incidence microscope with 5- μm spatial resolution, 500- μm -diameter field of view, and x-ray probe energy to 9 keV.
- Develop an XUV spectrometer with 200-ps time resolution and open beam optical coupling for dynamic materials properties studies.
- Develop the capability for fielding TREX time- and spatially-resolved x-ray spectrometers on up to four different lines-of-sight for z-pinch emission uniformity studies.
- Expand the neutron TOF system to include two neutron TOF detectors on-axis above and below the pinch, and two detectors on radial LOS pipes at 12° , located 180° apart azimuthally.

- Develop a target burn history diagnostic with 20-ps time resolution useful at yield levels of 10^{10} - 10^{12} neutrons in the bremsstrahlung and debris environment of ZR.
- Develop a target bang time diagnostic with 50-ps time resolution useful at yield levels of 10^{10} - 10^{12} neutrons in the bremsstrahlung and debris environment of ZR.
- Develop a neutron spectrometer with 100-keV resolution and 5×10^6 neutron detection threshold for fuel areal density $\langle \rho r \rangle$ measurements based on detection of secondary neutrons produced in pure deuterium fuel at $\langle \rho r \rangle$ values below 20 mg/cm^2 .
- Develop a visible imaging hydrotest system for studying the deformation of small structures mounted on the primary hohlraum.

Priority 3 Diagnostic Development

These are new diagnostics that appear to represent a useful enhancement to diagnostic capabilities on ZR, but whose utility, feasibility, or cost must be further investigated before a full commitment to development can be made. These diagnostics are not critical to ZR experiments in the near term, and may require significant advances in research areas such as ICF fuel capsule performance to be fully utilized.

- Develop a fuel areal density $\langle \rho r \rangle$ diagnostic for $\langle \rho r \rangle$ values greater than 20 mg/cm^2 based on detection of tertiary neutrons from DT thermonuclear reactions.
- Develop a neutron core imaging system with a spatial resolution of better than $50 \text{ }\mu\text{m}$ and a 500 - $1000 \text{ }\mu\text{m}$ field of view useful at yield levels of $> 10^{12}$ neutrons.
- Develop a pulsed power flash radiography system for deformation studies of magnetically-driven flyer plates and irradiated mechanical structures. It is possible that the ZBL backlighter may be able to perform part of this function.

VI.2. Budget for New Diagnostic Development

The following is an estimate of the investment in new diagnostics required for ZR to be funded by a request for additional program funds. It is assumed that ongoing improvements to existing core diagnostics will be funded within the envelope of the present budget.

Annual investment in new diagnostic development over 6 years (FY03 - FY08):

X-ray imaging (for ZBL, high resolution pinhole cameras, etc.)	\$ 500 k/yr
Spectroscopy (instruments, dedicated streak, framing cameras)	\$ 300 k/yr
Streak, framing cameras (facility-owned, shared)	\$ 200 k/yr
Neutron diagnostics	\$ 200 k/yr
Diagnostic infrastructure not covered within ZR Project	\$ 100 k/yr
Total/year	\$ 1.3 M
6 year total	\$ 7.8 M

Other diagnostic investment for ZR (FY03 - FY08):

Additional VISAR channels (FY03)	\$ 400 k
Streak camera for Bragg diffraction measurements (FY04)	\$ 200 k
DIM module (FY05)	\$ 1 M
DIM module (FY06)	\$ 1 M
Pulsed power flash radiography system (FY07)	\$ 500 k
Visible imaging hydrotest capability (FY08)	\$ 250 k
Total	\$ 3.35 M
Grand total	\$ 11.15 M

VII. Summary and Conclusions

This report presents a comprehensive plan for ZR diagnostic development covering the first few years of ZR operation. ZR will be a versatile machine, providing advanced capabilities for both pulsed x-ray production and high pressure generation. Recommendations presented here for new ZR diagnostic development cover a wide range of increasingly sophisticated diagnostics that will be required for complex physics experiments utilizing these advanced source capabilities. Recommended areas of concentration for new diagnostic development include x-ray imaging with the ZBL backlighter and with high-resolution x-ray framing pinhole cameras, spectroscopy covering a broad spectral range, low detection threshold neutron spectroscopy, advanced VISAR interferometry and shock breakout diagnostics for shock physics measurements, laser probing of low density, z-pinch-related plasmas, visible hydrotest imaging of secondary hohlraum structural deformations, and pulsed power flash radiography of rapidly moving structures. Requirements common to many of these development proposals include the need for survivable instruments with high spatial and temporal resolution, capable of low noise operation in the severe EMP, bremsstrahlung, and blast environments of ZR, reduced diagnostic trigger signal jitter, more and flexible diagnostic line-of-sight access, and the capability for efficient exchange of diagnostics with other laboratories.

If the essential recommendations of this ZR diagnostic development plan are carried out on a 4-6 year time scale starting in FY02, the resulting enhanced set of diagnostic capabilities will be adequate to meet the diverse programmatic needs of a broad range of defense, energy, and general science programs into the next decade.

Acknowledgements

The author would like to thank James R. Asay, James E. Bailey, Guy R. Bennett, David E. Bliss, Gordon A Chandler, Robert E. Chrien (LANL), Michael E. Cuneo, Jean-Paul Davis, Christopher Deeney, Michael D. Furnish, Clint A. Hall, Robert F. Heeter (LLNL), Randy J. Hickman, Daniel O. Jobe, Robert R. Johnston, Marcus D. Knudson, Ramon J. Leeper, Barbara A. Lewis, Michael G. Mazarakis, M. Keith Matzen, Dillon H. McDaniel, Thomas A. Mehlhorn, Jerry A. Mills, Thomas J. Nash, Dan S. Nielsen, Donald W. Petmecky, John L. Porter, Jr., David B. Reisman (LLNL), Gregory A. Rochau, Stephen D. Rothman (AWE), Laurence E. Ruggles, Carlos L. Ruiz, Johann F. Seamen, Thomas W. L. Sanford, Walter W. Simpson, Daniel B. Sinars, C. Shane Speas, William A. Stygar, Mary Ann Sweeney, Jose A. Torres, Robert G. Watt (LANL), Edward A. Weinbrecht, and David F. Wenger for many valuable suggestions and insights on the requirements for ZR diagnostic and infrastructure development.

Sandia is a multiprogram laboratory operated by Sandia Corporation, a Lockheed Martin Company, for the United States Department of Energy's National Nuclear Security Administration under Contract No. DE-AC04-94AL85000.

References

1. R. B. Spielman, C. Deeney, G. A. Chandler *et al.*, “Tungsten wire-array Z-pinch experiments at 200 TW and 2 MJ”, *Phys. Plasmas* **5**, 2105 (1998).
2. E. Weinbrecht *et al.*, “Statement of Mission Need and Project Description for Refurbishment of the Z Accelerator – ZR at Sandia National Laboratories”, Report to the U. S. Department of Energy, Sandia National Laboratories, 09/17/01.
3. “Sandia’s Pulsed Power Program: FY02 Implementation Plan”, Mary Ann Sweeney and Marshall Sluyter, eds., Draft Report, Sandia National Laboratories, May 2, 2002.
4. E. Weinbrecht *et al.*, “Preliminary Project Execution Plan for Refurbishment of the Z Accelerator at Sandia National Laboratories”, Report to the U. S. Department of Energy, Rev. 2.3, Sandia National Laboratories, 02/15/02.
5. G. R. Bennett, O. L. Landen, R. G. Adams, J. L. Porter, L. E. Ruggles, W. W. Simpson, C. Wakefield, “X-ray imaging techniques on Z using the Z-Beamlet laser”, *Rev. Sci. Instrum.* **72**, 657 (2001).
6. D. L. Hanson, R. A. Vesey, M. E. Cuneo *et al.*, “Measurement of radiation symmetry in Z-pinch-driven hohlraums”, *Phys. Plasmas* **9**, 2173 (2002).
7. G. R. Bennett, R. G. Adams, M. E. Cuneo *et al.*, “Z-Beamlet Point Projection X-ray Imaging of ICF Implosions in Z Accelerator Z-Pinch-Driven Hohlraums”, *Bull. Am. Phys. Soc.* **46**, 238 (2001).
8. D. C. Rovang, W. W. Simpson, L. E. Ruggles, J. L. Porter, “An Electronic Fast Shutter System for Debris Mitigation on Z”, *Digest of Technical Papers, 13th IEEE Int. Pulsed Power Conf., June 17-22, 2001, Las Vegas, Nevada* by IEEE Nuclear and Plasma Sciences Society, 2002.
9. M. E. Cuneo, R. A. Vesey, J. L. Porter, Jr. *et al.*, “Double Z-Pinch Hohlraum Drive with Excellent Temperature Balance for Symmetrical Inertial Confinement Fusion Capsule Implosions”, *Phys. Rev. Lett.* **88**, 215004 (2002).
10. G. R. Bennett, M. E. Cuneo, R. A. Vesey *et al.* “Symmetric Inertial-Confinement-Fusion-Capsule Implosions in a Double-Z-Pinch-Driven Hohlraum”, *Phys. Rev. Lett.* **89**, 245002 (2002).
11. R. A. Vesey, M. E. Cuneo, G. R. Bennett *et al.*, “Demonstration of Radiation Symmetry Control for Inertial Confinement Fusion in Double Z-Pinch Hohlraums”, *Phys. Rev. Lett.* **90**, 035005 (2003).
12. S. A. Slutz, M. R. Douglas, J. S. Lash, R. A. Vesey, G. A. Chandler, T. J. Nash, M. S. Derzon, “Scaling and optimization of the radiation temperature in dynamic hohlraums”, *Phys. Plasmas* **8**, 1673 (2001).
13. J. E. Bailey, G. A. Chandler, S. A. Slutz *et al.*, “X-ray Imaging Measurements of Capsule Implosions Driven by a Z-Pinch Dynamic Hohlraum”, *Phys. Rev. Lett.* **89**, 095004 (2002).
14. D. B. Sinars, G. R. Bennett, J. L. Porter, D. F. Wenger, “Evaluation of bent crystal backlighting and microscopy techniques for Z”, (submitted for publication, 2002).
15. Y. Aglitskiy, T. Lahecka, S. Obenshain *et al.*, “High-resolution monochromatic x-ray imaging system based on spherically bent crystals”, *Appl. Optics* **37**, 5253 (1998).
16. J. A. Koch, O. L. Landen, T. W. Barbee, Jr. *et al.*, “High-energy x-ray microscopy techniques for laser-fusion plasma research at the National Ignition Facility”, *Appl. Optics* **37**, 1784 (1998).

17. S. A. Pikuz, T. A. Shelkovenko, V. M. Romanova, D. A. Hammer, A. Yu. Faenov, V. A. Dyakin, T. A. Pikuz, “High-luminosity monochromatic x-ray backlighting using an incoherent plasma source to study extremely dense plasmas”, *Rev. Sci. Instrum.* **68**, 740 (1997).
18. S. A. Pikuz, T. A. Shelkovenko, V. M. Romanova, D. A. Hammer, A. Yu. Faenov, V. A. Dyakin, T. A. Pikuz, “Monochromatic x-ray probing of an ultradense plasma”, *JETP Lett.* **61**, 639 (1995).
19. F. J. Marshall, Q. Su, “Quantitative measurements with x-ray microscopes in laser-fusion experiments”, *Rev. Sci. Instrum.* **66**, 725 (1995).
20. F. J. Marshall, G. R. Bennett, “A high-energy x-ray microscope for inertial confinement fusion”, *Rev. Sci. Instrum.* **70**, 617 (1999).
21. F. J. Marshall, J. A. Oertel, “A framed monochromatic x-ray microscope for ICF”, *Rev. Sci. Instrum.* **68**, 735 (1997).
22. K. Fujita, H. Nishimura, I. Niki *et al.*, “Monochromatic x-ray imaging with bent crystals for laser fusion research”, *Rev. Sci. Instrum.* **72**, 744 (2001).
23. Y. Aglitsky, T. Lehecka, S. Obenshain, C. Pawley, C. M. Brown, J. Seely, “X-ray crystal imagers for inertial confinement fusion experiments”, *Rev. Sci. Instrum.* **70**, 530 (1999).
24. J. A. Oertel, T. Archuleta, C. G. Peterson, F. J. Marshall, “Dual microchannel plate module for a gated monochromatic x-ray imager”, *Rev. Sci. Instrum.* **68**, 789 (1997).
25. I. Uschmann, E. Forster, H. Nishimura, K. Fujita, Y. Kato, S. Nakai, “Temperature mapping of compressed fusion pellets obtained by monochromatic imaging”, *Rev. Sci. Instrum.* **66**, 734 (1995).
26. G. R. Bennett, “Advanced one-dimensional x-ray microscope for the Omega Laser Facility”, *Rev. Sci. Instrum.* **70**, 608 (1999).
27. R. Kodama, H. Shiraga, M. Miyanaga, T. Matsushita, M. Nakai, H. Azechi, K. Mima, Y. Kata, “Study of laser-imploded core plasmas with an advanced Kirkpatrick-Baez x-ray microscope”, *Rev. Sci. Instrum.* **68**, 824 (1997).
28. E. Forster, K. Gabel, I. Uschmann, “X-ray microscopy of laser-produced plasmas with the use of bent crystals”, *Laser Part. Beams* **9**, 135 (1991).
29. I. Uschmann, K. Fujita, I. Niki, R. Butzbach, H. Nishimura, J. Funakura, M. Nakai, E. Forster, K. Mima, “Time-Resolved Ten-Channel Monochromatic Imaging of Inertial Confinement Fusion Plasmas”, *Appl. Opt.* **39**, 5865 (2000).
30. J. A. Oertel, C. G. Peterson, “Los Alamos pinhole camera (LAPC): A new flexible x-ray pinhole camera”, *Rev. Sci. Instrum.* **68**, 786 (1997).
31. H. F. Robey, K. S. Budil, B. A. Remington, “Spatial resolution of gated x-ray pinhole cameras”, *Rev. Sci. Instrum.* **68**, 792 (1997).
32. O. L. Landen, A. Lobban, T. Tutt, P. M. Bell, R. Costa, D. R. Hargrove, F. Ze, “Angular sensitivity of gated microchannel plate framing cameras”, *Rev. Sci. Instrum.* **72**, 709 (2001).
33. R. E. Turner, O. L. Landen, D. K. Bradley, S. S. Alvarez, P. M. Bell, R. Costa, J. D. Moody, D. Lee, “Comparison of charge coupled device vs film readouts for gated micro-channel plate cameras”, *Rev. Sci. Instrum.* **72**, 706 (2001).
34. D. K. Bradley, P. M. Bell, O. L. Landen, J. D. Kilkenny, J. Oertel, “Development and characterization of a pair of 30-40 ps x-ray framing cameras”, *Rev. Sci. Instrum.* **66**, 716 (1995).

35. R. K. Reich, W. M. McGonagle, J. A. Gregory, R. W. Moutain, B. B. Kosicki, E. D. Savoye, "High performance charge-coupled-device imager technology for plasma diagnostics", *Rev. Sci. Instrum.* **68**, 922 (1997).
36. C. J. Keane, R. C. Cook, T. R. Dittrich, B. A. Hammel, W. K. Levedahl, O. L. Landen, S. Langer, D. H. Munro, H. A. Scott, "Diagnosis of pusher-fuel mix in spherical implosions using x-ray spectroscopy", *Rev. Sci Instrum.* **66**, 689 (1995).
37. V. Kantsyrev, B. Bauer, A. Shlyaptseva *et al.*, "Advanced x-ray and extreme ultraviolet diagnostics and first applications to x-pinch plasma experiments at the Nevada Terawatt Facility", *Rev. Sci. Instrum.* **72**, 663 (2001).
38. J. E. Bailey, A. L. Carlson, G. A. Chandler, C. A. Hall, D. L. Hanson, R. Johnston, P. Lake, J. Lawrence, "Optical spectroscopy measurements of shock waves driven by intense z-pinch radiation", *J. Quant. Spectr. and Rad. Transfer* **65**, 31 (2000); J. E. Bailey, D. Cohen, G. A. Chandler *et al.*, "Neon photoionization experiments driven by Z-pinch radiation", *J. Quant. Spectr. and Rad. Transfer* **71**, 157 (2001).
39. T. J. Nash, M. S. Derzon, G. A. Chandler *et al.*, "Diagnostics on Z", *Rev. Sci. Instrum.* **72**, 1167 (2001).
40. T. J. Nash, M. S. Derzon, G. A. Chandler *et al.*, "Axial diagnostic package for Z", *Rev. Sci. Instrum.* **70**, 464 (1999).
41. M. D. Knudson, D. L. Hanson, J. E. Bailey, C. A. Hall, J. A. Asay, W. W. Anderson, "Equation of State Measurements in Liquid Deuterium to 70 Gpa", *Phys. Rev. Lett.* **87**, 225501 (2001).
42. M. D. Knudson, D. L. Hanson, J. E. Bailey, C. A. Hall, J. A. Asay, "Use of a Wave Reverberation Technique to Infer the Density Compression of Shocked Liquid Deuterium to 75 Gpa", *Phys. Rev. Lett.* **90**, 035505 (2003).
43. L. E. Ruggles, J. L. Porter, R. Bartlett, "Calibration of a time-resolving spectrometer in the 100-800 eV spectral region", *Rev. Sci. Instrum.* **68**, 1063 (1997).
44. D. D. Ryutov, M. S. Derzon, M. K. Matzen, "The Physics of Fast Z Pinches", *Rev. Mod. Phys.* **72**, 167 (2000).
45. K. Moy, Special Technologies Laboratory, Bechtel-Nevada, and M. E. Cuneo, Sandia National Laboratories, private communication (2002).
46. R. J. Leeper, G. A. Chandler, G. W. Cooper *et al.*, "Target diagnostic system for the National Ignition Facility", *Rev. Sci. Instrum.* **68**, 868 (1997).
47. T. J. Murphy, C. W. Barnes, R. R. Berggren *et al.*, "Nuclear diagnostics for the National Ignition Facility", *Rev. Sci. Instrum.* **72**, 773 (2001).
48. G. W. Cooper, C. L. Ruiz, "NIF total neutron yield diagnostic", *Rev. Sci. Instrum.* **72**, 814 (2001).
49. C. W. Barnes, T. J. Murphy, J. A. Oertel, "High-yield neutron activation system for the National Ignition Facility", *Rev. Sci. Instrum.* **72**, 818 (2001).
50. T. J. Murphy, J. L. Jimerson, R. R. Berggren, J. R. Faulkner, J. A. Oertel, P. J. Walsh, "Neutron time-of-flight and emission time diagnostics for the National Ignition Facility", *Rev. Sci. Instrum.* **72**, 850 (2001).
51. N. Izumi, K. Yamaguchi, T. Yamgajo, T. Kasai, T. Urano, H. Azechi, S. Nakai, T. Iida, "A highly efficient neutron time-of-flight detector for inertial confinement fusion experiments", *Rev. Sci. Instrum.* **70**, 1221 (1999).
52. S. E. Caldwell, S. S. Han, J. R. Joseph, T. L. Petersen, C. S. Young, "Burn history measurements in laser based fusion", *Rev. Sci. Instrum.* **68**, 603 (1997).

53. J. A. Frenje, K. M. Green, D. G. Hicks *et al.*, “A neutron spectrometer for precise measurements of DT neutrons from 10 to 18 MeV at OMEGA and the National Ignition Facility”, *Rev. Sci. Instrum.* **72**, 854 (2001).
54. D. C. Wilson, T. J. Murphy, W. C. Mead, L. Disdier, M. Houry, C. Bayer, J. –L. Bourgade, “Scattered and (n, 2n) neutrons as a measure of areal density in ICF capsules”, *Bull. Am. Phys. Soc.* **46**, 290 (2001).
55. N. Izumi, R. A. Lerche, T. W. Phillips, G. J. Schmid, M. J. Moran, S. P. Hatchett, T. C. Sangster, “Conceptual design of a scintillator fiber neutron detector for rho-R measurements in ICF”, *Bull. Am. Phys. Soc.* **46**, 290 (2001).
56. G. J. Schmid, V. Yu. Glebov, S. P. Hatchett *et al.*, “CVD diamond detector for DD rho-r measurement at OMEGA/NIF”, *Bull. Am. Phys. Soc.* **46**, 290 (2001).
57. M. B. Nelson, M. D. Cable, “LaNSA: A large neutron scintillator array for neutron spectroscopy at NOVA”, *Rev. Sci. Instrum.* **63**, 4874 (1992).
58. G. L. Morgan, R. R. Berggren, P. A. Bradley *et al.*, “Development of a neutron imaging diagnostic for inertial confinement fusion experiments”, *Rev. Sci. Instrum.* **72**, 865 (2001).
59. R. A. Lerche, N. Izumi, T. C. Sanapter, R. K. Fisher, J. L. Bourgade, O. Delage, L. Disdier, A. Rouyer, P. A. Jaanimagi, “Bubble Detectors for High Resolution, Low Magnification Neutron Imaging”, *Bull. Am. Phys. Soc.* **46**, 238 (2001).
60. R. A. Lerche, N. Izumi, T. C. Sanapter, R. K. Fisher, J. L. Bourgade, O. Delage, L. Disdier, A. Rouyer, P. A. Jaanimagi, “Bubble Detectors for High Resolution, Low Magnification Neutron Imaging”, *Bull. Am. Phys. Soc.* **46**, 238 (2001).
61. R. A. Lerche, D. Ress, R. J. Ellis, S. M. Lane, K. N. Nugent, “Neutron penumbral imaging of laser-fusion targets”, *Laser Part. Beams* **9**, 99 (1991).
62. D. L. Hanson, M. D. Knudson, C. A. Hall, J. R. Asay, J. E. Bailey, R. W. Lemke, J. P. Davis, R. B. Spielman, B. V. Oliver, D. B. Hayes, “Precision Shock Physics Capabilities for Inertial Fusion Studies using the Z Accelerator Current Drive”, *Inertial Fusion Sciences and Applications 2001*, K. A. Tanaka, D. D. Meyerhofer, J. Meyer-ter-Vehn, eds. (Paris: Elsevier, 2002) pp. 1091-1095.
63. C. A. Hall, “Isentropic compression experiments on the Sandia Z accelerator”, *Phys. Plasmas* **7**, 2069 (2000); C. A. Hall, J. R. Asay, M. D. Knudson, W. A. Stygar, R. B. Spielman, T. D. Pointon, D. B. Reisman, A. Toor, R. C. Cauble, “Experimental configuration for isentropic compression of solids using pulsed magnetic loading”, *Rev. Sci. Instrum.* **72**, 1 (2001).
64. L. M. Barker, R. E. Hollenbach, “Laser interferometer for measuring high velocities of any reflecting surface”, *J. Appl. Phys.* **43**, 4669 (1972).
65. J. F. Camacho, S. M. Cameron, D. E. Bliss, J. S. DeGroot, “Characterization of a Laser-Generated Plasma using Collective Thomson Scattering and Schlieren Imaging”, *Bull. Am. Phys. Soc.* **46**, 238 (2001).
66. V. V. Aleksandrov, A. V. Branitskii, G. S. Volkov *et al.*, “Dynamics of Heterogeneous Liners with Prolonged Plasma Creation”, *Plasma Phys. Reports* **27**, 89 (2001).
67. R. B. Spielman, C. Deeney, D. L. Fehl, D. L. Hanson, N. R. Keltner, J. S. McGurn, J. L. McKenney, “Fast resistive bolometry”, *Rev. Sci. Instrum.* **70**, 651 (1999).
68. G. A. Chandler, C. Deeney, M. Cuneo *et al.*, “Filtered x-ray diode diagnostics fielded on the Z accelerator for source power measurements”, *Rev. Sci. Instrum.* **70**, 561 (1999).

69. R. B. Spielman, "Diamond photoconducting detectors as high power z-pinch diagnostics", *Rev. Sci. Instrum.* **66**, 867 (1995).
70. R. B. Spielman, L. E. Ruggles, R. E. Pepping, S. E. Breeze, J. S. McGurn, and K. W. Struve, "Fielding and calibration issues for diamond photoconducting detectors", *Rev. Sci. Instrum.* **68**, 782 (1997).
71. R. E. Turner, O. L. Landen, P. Bell, R. Costa, D. Hargrove, "Achromatically filtered diamond photoconductive detectors for high power soft x-ray flux measurements", *Rev. Sci. Instrum.* **70**, 656 (1999).
72. W. A. Stygar, Sandia National Laboratories, TEP diagnostic, private communication (2002).
73. D. L. Fehl, D. J. Muron, R. J. Leeper, G. A. Chandler, C. Deeney, W. A. Stygar, R. B. Spielman, "Absolute, soft x-ray calorimetry on the Z facility at Sandia National Laboratories", *Rev. Sci. Instrum.* **70**, 270 (1999).
74. B. Afeyan, M. Cuneo, R. B. Spielman, "Wavelet Denoising of and X-Ray Power Extraction from Bolometry Data from Fast Z Pinches", *Bull. Am. Phys. Soc.* **46**, 235 (2001).
75. W. A. Stygar, R. B. Spielman, H. G. Ives *et al.*, "D-dot and B-dot Monitors for Z-Vacuum-Section Power-Flow Measurements", *Proc. of 11th IEEE International Pulsed Power Conference (1997)*, p. 1258..
76. W. A. Stygar, Sandia National Laboratories, new load current monitor array, private communication (2002).
77. B. L. Henke, H. T. Yamada, T. J. Tanaka, "Pulsed plasma source spectroscopy in the 80-8000 eV x-ray region", *Rev. Sci. Instrum.* **54**, 1311 (1983).
78. T. Nash, M. Derzon, R. Leeper, D. Jobe, M. Hurst, J. Seamen, "Spatially and temporally resolved crystal spectrometer for diagnosing high temperature pinch plasmas on Z", *Rev. Sci. Instrum.* **70**, 302 (1999).
79. R. F. Heeter, J. E. Bailey, M. E. Cuneo, J. Emig, M. E. Foord, P. T. Springer, R. S. Thoe, "Plasma diagnostics for x-ray driven foils at Z", *Rev. Sci. Instrum.* **72**, 1224 (2001).
80. J. R. Kimbrough, P. M. Bell, G. B. Christianson, F. D. Lee, D. H. Kalantar, T. S. Perry, N. R. Sewall, A. J. Wootton, "National Ignition Facility core x-ray streak camera", *Rev. Sci. Instrum.* **72**, 748 (2001).
81. D. H. Kalantar, P. M. Bell, T. S. Perry, N. Sewall, J. Kimbrough, F. Weber, C. Diamond, K. Piston, "Optimizing data recording for the NIF core diagnostic x-ray streak camera", *Rev. Sci. Instrum.* **72**, 751 (2001).
82. R. Kodama, K. Okada, Y. Kato, "Development of a two-dimensional space-resolved high speed sampling camera", *Rev. Sci. Instrum.* **70**, 625 (1999).
83. H. Shiraga, M. Nakasuji, M. Heya, N. Miyanaga, "Two-dimensional sampling-image x-ray streak camera for ultrafast imaging of inertial confinement fusion plasmas", *Rev. Sci. Instrum.* **70**, 620 (1999).
84. N. Miyanaga, N. Ohba, K. Fujimoto, "Fiber scintillator/streak camera detector for burn history measurement in inertial confinement fusion experiment", *Rev. Sci. Instrum.* **68**, 621 (1997).
85. H. Shiraga, N. Miyanaga, M. Heya, M. Nakasuji, Y. Aoki, H. Azechi, T. Yamanaka, K. Mima, "Ultrafast two-dimensional x-ray imaging with x-ray streak cameras for laser fusion research", *Rev. Sci. Instrum.* **68**, 745 (1997).
86. H. Shiraga, M. Heya, M. Nakasuji, N. Miyanaga, H. Azechi, H. Takabe, T.

- Yamanaka, K. Mima, “One- and two-dimensional fast x-ray imaging of laser-driven implosion dynamics with x-ray streak cameras”, *Rev. Sci. Instrum.* **68**, 828 (1997).
87. W. J. Hibbard, M. D. Landon, M. D. Vergino, F. D. Lee, “Design of the National Ignition Facility diagnostic instrument manipulator”, *Rev. Sci. Instrum.* **72**, 530 (2001).
88. M. J. Hurst, T. J. Nash, M. Derzon, J. W. Kellogg, J. Torres, J. McGurn, J. Seamen, D. Jobe, S. E. Lazier, “Fielding of the on-axis diagnostic package at Z”, *Rev. Sci. Instrum.* **70**, 468 (1999).
89. M. Tabak, J. Hammer, M. E. Glinsky, W. L. Krauer, S. C. Wilks, J. Woodworth, E. M. Campbell, M. D. Perry, “Ignition and high gain with ultrapowerful lasers”, *Phys. Plasmas* **1**, 1626 (1994).
90. R. Kodama, P. A. Norreys, K. Mima *et al.*, “Fast heating of ultrahigh-density plasma as a step towards laser fusion ignition”, *Nature* **412**, 798 (2001).
91. R. Kodama, H. Shiraga, K. Shigemori *et al.*, “Fast heating scalable to laser fusion ignition”, *Nature* **418**, 933 (2002).
92. T. E. Cowan, M. Roth, J. Johnson *et al.*, “Intense electron and proton beams for PetaWatt laser-matter interactions”, *Nucl. Instrum. Methods* **A455**, 130 (2000).
93. M. H. Key, E. M. Campbell, T. E. Cowan *et al.*, “Studies of the Relativistic Electron Source and Related Phenomena in Petawatt Laser Matter Interactions”, *Inertial Fusion Sciences and Applications* 99, C. Labaune, W. J. Hogan, K. A. Tanaka, eds. (Paris:Elsevier, 2000) pp. 392-400.
94. R. A. Snavely, M. H. Key, S. P. Hatchett *et al.*, “Intense High-Energy Proton Beams from Petawatt-Laser Irradiation of Solids”, *Phys. Rev. Lett.* **85**, 2945 (2000).
95. S. Atzeni, “Inertial fusion fast ignitor: Igniting pulse parameter window vs. the penetration depth of heating particles and the density of the precompressed fuel”, *Phys. Plasmas* **6**, 3316 (1999).
96. S. A. Slutz, M. C. Herrmann, “Radiation driven capsules for fast ignition fusion”, *Phys. Plasmas* **10**, 234 (2003).
97. D. L. Hanson, R. A. Vesey, S. A. Slutz *et al.*, “Hemispherical Capsule Implosion Measurements in a Z-Pinch-Driven Fast Ignitor Fuel Compression Geometry”, *Bull. Am. Phys. Soc.* **47**, 219 (2002).
98. B. L. Henke *et al.*, *J. Opt. Soc. Am.* **B3**, 1540 (1986).

Appendix A. Summary of Z Core Diagnostics

A1. List of Radial (12°) Diagnostics

LOS 1/2 (Developmental diagnostic LOS)	Grazing incidence x-ray streak camera Time-resolved grazing incidence x-ray pinhole camera
LOS 5/6	Bolometer array XRD array PCD array TEP or calorimeter diagnostic TGS
LOS 9/10	Large format time-resolved x-ray pinhole camera
LOS 13/14	Time-integrated x-ray crystal spectrometers (2) Time-resolved x-ray crystal spectrometers (2)
LOS 17/18	TGS Time-resolved x-ray pinhole camera Si diode array
LOS 21/22	Bolometer array XRD array PCD array
LOS 25/26	Neutron TOF diagnostic
LOS 29/30	TGS Time-resolved x-ray pinhole camera Si diode array
LOS 33/34	TREX

A2. List of Axial (81°- 90°) Diagnostics (Axial diagnostics package may vary)

LOS Center (90°)	Time-resolved x-ray pinhole camera or TREX
LOS 1:30 (81°)	Not used at present
LOS 3:00 (84°)	Time-resolved x-ray pinhole camera

LOS 4:30 (81°)	Time-integrated x-ray crystal spectrometer
LOS 4:30 (86°)	EST diagnostic
LOS 6:00 (84°)	XRD array
LOS 7:30 (81°)	PCD array
LOS 9:00 (84°)	Time-resolved x-ray pinhole camera or TREX
LOS 10:30 (81°)	Time-resolved x-ray crystal spectrometer
LOS 12:00 (84°)	Bolometer array

A3. List of Target Chamber (Close-in) Diagnostics

ZBL backlighter diagnostic system

ASBO diagnostic (open beam)

ASBO diagnostics (fiber-optic-coupled)

Single-point VISARs

Line VISAR

Visible spectrometers

EST/PST diagnostic

Neutron activation diagnostics

Laser probe diagnostics

A4. List of Electrical Power Flow Diagnostics

Load current monitors

MITL current monitors

Insulator stack current and voltage monitors

A5. Brief Description of Diagnostics

Grazing-incidence x-ray streak camera (LOS 1/2) - under development

This instrument is able to record a continuous time-history for up to 33 ns of emission in a narrow spectral band with one-dimensional spatial resolution. It has been used to look at emission from a stagnating z pinch with spatial resolution in the horizontal direction and at emission from targets above the z pinch. At present, the instrument consists of a Kentech x-ray streak camera and image intensifier paired with a 2° SiO₂ mirror in ~ 1:1 magnification geometry. If used with a Ti filter, the filter transmission, Au photocathode sensitivity, and mirror reflectivity combine to select a narrow spectral band from about 375 eV to 450 eV. This camera could be coupled to a crystal spectrometer to obtain time-resolved spectra for ZR experiments.

Grazing-incidence gated pinhole camera (LOS 1/2) - under development

This camera is being developed to measure aperture hole closure and study the implosion or burnthrough of ICF targets imaged by self-emission in a narrow spectral range. It consists of a 4-frame, gated MCP pinhole camera system paired with a 2° SiO₂ mirror in ~ 1:1 magnification geometry, with a spectral response in the range of 375 to 450 eV, eliminating uncertainties introduced by the more broadband response of filtered x-ray pinhole cameras.

Bolometer array

Bolometers are the primary total x-ray yield diagnostic on Z for soft x-rays in the range from 10-1500 eV. A constant current is passed through an unfiltered 1- μ m-thick nickel film on a low thermal diffusivity substrate. The resistive voltage change resulting from film heating by x-ray energy deposition is proportional to the absorbed fluence. When fitted with magnets to provide a transverse magnetic field to suppress photoelectron emission from the metal film, bolometers are time resolved, with response time on the order of 1 ns. Because of signal noise problems in the past, bolometers have not generally been used directly for x-ray power measurements on Z. Integrals of x-ray diode waveforms are typically normalized to the bolometer yield to obtain pinch power waveforms and hohlraum wall temperatures. An array of 3 fully-characterized bolometer elements may be fielded to obtain cross-calibration statistics.

Calorimeter

The calorimeter is a time-integrated fluence diagnostic for the measurement of total x-ray yield from z-pinch implosions. X-ray fluence is determined from a measurement of the temperature change of the calorimeter element resulting from x-ray absorption.

XRD array

Filtered x-ray diodes are used to measure x-ray power in various spectral cuts up to about 1.5 keV. X-ray power is determined from the photoelectron current emitted from a vitreous carbon cathode and collected by a biased anode screen. Pinch power and hohlraum wall temperatures are typically determined from XRD measurements by normalizing the integral of the 250 eV XRD channel to the nickel bolometer yield. Filtered five-channel and three-channel XRD arrays are currently fielded on Z.

PCD array

Diamond photoconducting detectors are a primary x-ray flux diagnostic on Z for higher energy (> 1 keV) x-rays. They feature fast, stable, flat response out to about 6 keV with a rugged, readily cleanable surface and very limited sensitivity to bremsstrahlung radiation. A filtered six-channel PCD array covering the x-ray energy range from 1-6 keV is used to estimate the shape of the free-bound continuum and to derive a time-resolved electron temperature for z-pinch.

TEP diagnostic

The Total Energy and Power diagnostic is a time-resolved z-pinch power diagnostic covering the x-ray energy range of 100 eV to 4 keV. The TEP consists of an array of 4 pinhole-apertured silicon photodiodes. Pinhole imaging reduces the incident flux on the detectors by a factor of 3000, allowing the instrument to measure peak pinch power levels up to 350 TW at a reasonable standoff distance, rather than being restricted to measurements in the early run-in phase of the z-pinch implosion.

TGS

The transmission grating spectrometer is used to measure the time-resolved spectrum of an x-ray source. The instrument consists of a transmission grating which disperses photons between 250 and 1000 eV onto a detector array of 16 silicon photodiodes. By fitting a Planckian to the TGS spectrum, the radiated power from a z-pinch or hohlraum wall can be determined with better accuracy than with the bolometer/XRD normalization method.

Pinhole-imaged silicon photodiode array

Each filtered photodiode in the pinhole-imaged silicon diode array is aligned with its own pinhole to view the same limited area of an x-ray source. A time-resolved source radiation temperature can be unfolded from the photodiode signals. An important application for this diagnostic is in the measurement of hohlraum wall reemission temperatures. Measurements can be made over a limited area at the center of a hohlraum aperture without the necessity of corrections for plasma hole closure.

Time-resolved x-ray pinhole camera

Time-resolved x-ray pinhole cameras are used on Z to measure hole closure of hohlraum apertures and to study the implosion or burnthrough of ICF targets imaged by self-emission. In a typical configuration, images are recorded on film with a four-frame gated MCP x-ray pinhole camera operated at magnification $M=1$ with a 1 ns gate time and 2 ns interframe time. Each frame has four 6x6 mm filtered pinhole images for each of four energy cuts. Another version of the framing pinhole camera has been developed with 8 frames, each with two 8x8 mm images. With a 100 μm pinhole required for adequate sensitivity at 9 m, the spatial resolution of the pinhole camera is about 200 μm .

Large format time-resolved x-ray pinhole camera

The large format pinhole camera is used to record detailed images of x-ray emission during z-pinch stagnation. The images are recorded on film with a detector consisting of nine 2x3 cm MCPs with a 100 ps gate to freeze motional blurring up to pinch velocities of 1×10^8 cm/s. The camera is typically operated at magnification 1.7 with 75 μm spatial resolution. The camera can be reconfigured to image pellet implosions at magnification 5.

EST diagnostic

The Energy, Space, and Time (EST) diagnostic measures time- and one-dimensional space-resolved x-ray/visible light emission in two spectral cuts. This imaging diagnostic for wire array implosion dynamics can be mounted close-in at 0° polar angle, within 1 m of the source, or on-axis, and at any azimuthal angle. The x-ray source is slit-imaged onto a filtered scintillator and the resulting visible light is fiber-optically coupled through a 1D array of 120 fibers to a streak camera.

Time-integrated x-ray crystal spectrometers

The time-integrated convex cylindrical x-ray spectrometers with slit-defined 1D spatial resolution of 100 μm – 1 mm and a film-based detector system cover a range of 1 – 10 keV with spectral resolution of $\lambda/\Delta\lambda = 500$ limited by source broadening. KAP crystals with 2.5 cm curvature are used to record spectra from 1–4 keV and mica crystals in third or fifth order are used for 3-10 keV spectra.

Time-resolved x-ray crystal spectrometers

The time-resolved, spatially-integrated convex crystal x-ray spectrometers use an MCP framing camera with film as a detector. Temporal resolution is achieved with seven MCP striplines gated for 1-2 ns. The spectral range for the KAP or mica crystals is more limited than for the time-integrated instruments because of the 4 cm length of the MCPs.

TREX

The TREX instrument is a time-resolved x-ray crystal spectrometer with 1D slit-defined spatial resolution and a detector system consisting of a six-frame MCP camera. The TREX is used for end-on and for radially- and axially-resolved side-on measurements of dynamic hohlraum capsule implosion symmetry by recording time- and spatially-resolved argon spectra from deuterium capsule implosions with argon seed gas.

Visible spectrometers

Streaked visible and UV spectroscopy in the range between 270 and 1000 nm is used to study z-pinch wire plasma initiation, preheat in on-axis foams, and temperatures in shock-heated liquid deuterium, among other applications. Visible light is fiber-optically coupled to the spectrometers, time-resolved with a streak camera, and recorded on film. Spectral range and resolution are determined by the grating selection, ranging from 150 to 24000 grooves/mm.

Neutron TOF diagnostic

The neutron time-of-flight detector presently on Z is intended for use on ICF fuel pellet implosion shots with moderate total neutron yields in the 10^8 - 10^{10} range. Neutron TOF measurements of the energy broadening of DD and DT thermonuclear neutrons can determine both the neutron total yield and the fusion burn ion temperature. The scintillator-PM tube neutron detector for this instrument is heavily shielded against bremsstrahlung background but collimated to view the z-pinch load region, which is the source of significant bremsstrahlung radiation.

Neutron activation diagnostics

Total neutron yields above about 10^8 neutrons can be measured using nuclear activation techniques, with activation samples located within the Z target chamber. Indium 115 is used to measure the 2.45 MeV neutrons from the DD fusion reaction by the inelastic neutron scattering reaction $^{115}\text{In}(n,n')^{115\text{m}}\text{In}$ with a threshold of 336 keV. The In 115m metastable state has a half-life of 4.49 h and emits a 336 keV gamma ray. Copper 63 is used to measure the 14.1 MeV neutrons from the DT fusion reaction by the neutron pickup reaction $^{63}\text{Cu}(n,2n)^{62}\text{Cu}(\beta^+)$ with a threshold of 11 MeV. The ^{62}Cu activation products with a half-life of 9.74 min are detected by measuring the 511 keV annihilation gamma rays.

ZBL backlighter diagnostic system

The Z-Beamlet laser backlighter system is a new diagnostic tool for point-projection and area x-ray backlighting with wide application to experiments on Z. At present, ZBL can produce about 500 J of 2ω laser energy in a 600 ps pulse focused to a 50 μm spot on an Fe target foil to generate 6.7 keV x rays for point-projection imaging of ICF implosion capsules. A heavily-shielded low noise film-based x-ray detector with an electromagnetically-driven debris shutter has been developed to record backlit images of capsule implosions.

ASBO diagnostic (open beam)

The active shock breakout diagnostic can measure the shock velocity in a metal sample whose rear surface is not heated sufficiently for shock arrival to be detected by self-emission or fiber compression. In the open beam ASBO diagnostic, the light from an open beam probe laser is reflected off the polished rear surface of a step or wedge target forming part of a hohlraum wall, transported by open beam, and slit-imaged in 1-D onto a streak camera. Shock breakout is marked by a loss of reflectivity of the sample surface. The time difference between shock breakout at two points separated by a known thickness of material defines the shock velocity from which the radiation drive temperature can be derived.

ASBO diagnostics (fiber-optic-coupled)

Shock breakout can be observed at a large number of points on a sample using paired fiber-optic-coupled ASBO probes. A send fiber in each pair illuminates a small spot on the polished surface with laser light and a receive fiber collects some fixed fraction of the reflected light. The variation in intensity of fiber-optic-coupled light from the array of ASBO probes is then recorded with a streak camera. The resulting shock velocity data can provide a measure of the intensity and uniformity of the radiation drive over a sample.

Single-point VISARs

The Velocity Interferometric System for Any Reflector consists of a laser source, an interferometer for the reflected light, and a streak camera. For single-point operation, the laser probe beam and reflected light are fiber-optic-coupled to the VISAR. The Doppler shift of the reflected light, measured by an interferometer with a time delay between the reflected and reference beams, determines the time-resolved particle velocity at the rear surface of a shocked sample. The shock breakout time, marked by a sharp change in intensity of reflected light, can also be used to determine the shock velocity through a step or wedge surface. Multiple fiber-optic-coupled VISAR probes can be fielded on a single experiment for dynamic material properties studies.

Line VISAR

The line VISAR provides a 1D spatially-resolved interference pattern from which time-resolved particle and shock velocities can be determined continuously along a line across a sample. For the line VISAR, the laser probe and reflected light beams are transported by open beam.

Load current monitors

Typically, 2 to 4 calibrated cavity B-dot monitors are mounted on the anode surface about 5 cm from the z-pinch load axis to measure the total Z machine current. The B-dot monitors must be oriented azimuthally so their connectors/cables do not block any radial diagnostic LOS. A new load current diagnostic consisting of an array of eight calibrated B-dot monitors at the bottom of a magnetically insulated azimuthal anode

groove is being developed. This arrangement will smooth the current distribution, shield the B-dots from direct electron strikes, and provide improved accuracy through multiple measurements.

MITL current monitors

Twenty-four magnetically-insulated transmission line (MITL) B-dots are fielded on each shot. These measure the current in each of the four MITLs at a radius of 80 cm.

Insulator stack current and voltage monitors

B-dot current monitors and V-dot voltage monitors are fielded at the insulator stack to measure the current and voltage in each stack level at a radius of 165 cm.



Distribution

- 3 U. S. Department of Energy
Attn: Christopher J. Keane
Ralph Schneider
Richard Thorpe
1000 Independence Ave.
Washington, DC 20585
- 4 Los Alamos National Laboratory
Attn: Allan Hauer MS E527
Robert E. Chrien MS B220
George Idzorek
Robert G. Watt
P. O. Box 1663
Los Alamos, NM 87545
- 3 Lawrence Livermore National Laboratory
Attn: Bruce A. Hammel MS L-481
Robert F. Heeter MS L-043
David B. Reisman MS L-041
P. O. Box 808
Livermore, CA 94550
- 1 Laboratory for Laser Energetics
University of Rochester
Attn: Robert L. McCrory
250 E. River Road
Rochester, NY 14623
- 1 Naval Research Laboratory
Plasma Physics Division
Attn: Stephen P. Obenschain Code 6730
4555 Overlook Ave. SW
Washington, DC 20375
- 1 General Atomics
Attn: Joseph D. Kilkenny
P. O. Box 85608
San Diego, CA 92186-5608
- 1 Stephen D. Rothman
49 Burney Bit
Pamber Heath, Tadley, Hants
RG26 3TL England

1 University of New Mexico
Dept. of Chemistry and Nuclear Engineering
Attn: Prof. Gary W. Cooper
Albuquerque, NM 87183

1 MS 1190 Jeffrey P. Quintenz, 1600
1 MS 1190 Craig Olson, 1600
1 MS 1178 Douglas D. Bloomquist, 1630
1 MS 1178 Edward A. Weinbrecht, 1635
1 MS 1178 Guy L. Donovan, 1636
1 MS 1192 Mark L. Harris, 1636
1 MS 1192 Barbara A. Lewis, 1636
1 MS 1192 Jerry A. Mills, 1636
1 MS 1192 Donald W. Petmecky, 1636
1 MS 1192 James E. Potter, 1636
1 MS 1178 Finis W. Long, 1637
1 MS 1178 Debra A. Tabor, 1637
1 MS 1178 David L. Kitterman, 1639
1 MS 1178 Harry C. Ives, 1639
1 MS 1194 Dillon H. McDaniel, 1640
1 MS 1194 Kenneth W. Struve, 1644
1 MS 1194 David E. Bliss, 1644
1 MS 1194 William E. Fowler, 1644
1 MS 1194 Michael G. Mazarakis, 1644
1 MS 1194 John S. McGurn, 1644
1 MS 1194 Tim C. Wagoner, 1644
1 MS 1181 Christopher Deeney, 1646
1 MS 1181 Jean-Paul Davis, 1646
1 MS 1181 Randy J. Hickman, 1646
1 MS 1181 Marcus D. Knudson, 1646
1 MS 1181 P. David LePell, 1646
1 MS 1181 Joshua Mason, 1646
1 MS 1168 Lalit C. Chhabildas, 1647
1 MS 1168 Michael D. Furnish, 1647
1 MS 1168 Clint A. Hall, 1647
2 MS 1191 M. Keith Matzen, 1670
1 MS 1186 Johann F. Seamen, 1671
1 MS 1186 Terrance L. Gilliland, 1671
1 MS 1186 John L. McKenney, 1671
1 MS 1186 Diana G. Schroen, 1671
1 MS 1193 John L. Porter, 1673
1 MS 1193 Richard G. Adams, 1673
1 MS 1193 Guy R. Bennett, 1673
1 MS 1193 Michael E. Cuneo, 1673
20 MS 1193 David L. Hanson, 1673
1 MS 1193 Drew W. Johnson, 1673
1 MS 1193 Keith L. Keller, 1673

1	MS 1193	Larry E. Ruggles, 1673
1	MS 1193	Johann J. Seamen, 1673
1	MS 1193	Walter W. Simpson, 1673
1	MS 1193	Daniel B. Sinars, 1673
1	MS 1193	C. Shane Speas, 1673
1	MS 1193	Mark F. Vargas, 1673
1	MS 1193	David F. Wenger, 1673
1	MS 1186	Thomas A. Mehlhorn, 1674
1	MS 1196	Ramon J. Leeper, 1677
1	MS 1196	James E. Bailey, 1677
1	MS 1196	Alan L. Carlson, 1677
1	MS 1196	Gordon A. Chandler, 1677
1	MS 1196	Daniel O. Jobe, 1677
1	MS 1196	Patrick W. Lake, 1677
1	MS 1196	Steven E. Lazier, 1677
1	MS 1196	Raymond C. Mock, 1677
1	MS 1196	Thomas J. Nash, 1677
1	MS 1196	Daniel S. Nielsen, 1677
1	MS 1196	Richard E. Olson, 1677
1	MS 1196	Gregory A. Rochau, 1677
1	MS 1196	Carlos L. Ruiz, 1677
1	MS 1196	Thomas W. L. Sanford, 1677
1	MS 1196	William A. Stygar, 1677
1	MS 1196	Jose A. Torres, 1677
1	MS 9018	Central Technical Files, 8945-1
2	MS 0899	Technical Library, 9616